Development of a Robust Cyclic Plasticity Model and its Application to Soil-Structure Interaction Problems

by

Md. Raquibul Hossain

MASTER OF SCIENCE IN CIVIL ENGINEERING (STRUCTURE)

Department of Civil Engineering

BANGLADESH UNIVERSITY OF ENGINEERING AND TECHNOLOGY

September 2007

The thesis titled **"Development of a Robust Cyclic Plasticity Model and its Application to Soil-Structure Interaction Problems"** Submitted by **Md. Raquibul Hossain, Roll: 100504301(P), Session: October 2005,** has been accepted as satisfactory in partial fulfillment of the requirement for the degree of Master of Science in Civil Engineering (Structure) on 26st September, 2007.

BOARD OF EXAMINERS

Dr. Syed Ishtiaq Ahmad Associate Professor Department of Civil Engineering BUET, Dhaka.	Chairman
Dr. Md. Saiful Alam Siddiquee Professor Department of Civil Engineering BUET, Dhaka.	Member (Co-Supervisor)
Dr. Muhammad Zakaria Professor & Head Department of Civil Engineering BUET, Dhaka.	Member (Ex-officio)
Dr. M. Shamim Z. Bosunia Professor Department of Civil Engineering BUET, Dhaka.	Member
Dr. Iftekhar Anam Associate Professor The University of Asia Pacific	Member (External)

CANDIDATE'S DECLARATION

It is hereby declared that this thesis or any part of it has not been submitted elsewhere for the award of any degree or diploma.

M. R. Hossain

September, 2007 **Md. Raquibul Hossain**

This thesis is dedicated to my family. Their continuous inspirations made this effort possible.

TABLE OF CONTENTS

LIST OF FIGURES

LIST OF TABLES

ACKNOWLEDGMENTS

Thanks to Almighty Allah for His graciousness, unlimited kindness and with the blessings of Whom the good deeds are fulfilled.

I would like to express my deepest sincere gratitude to my supervisor Dr. Syed Ishtiaq Ahmad and my co-supervisor Dr. Md. Saiful Alam Siddiquee, for giving me a unique opportunity to work on such an important topic. Their continuous guidance, invaluable suggestions, affectionate encouragement, generous help and invaluable acumen are greatly acknowledged. Their keen interest on the topic and enthusiastic support on my effort was a source of inspiration to carry out the research. I consider myself fortunate to work under their supervision.

I express my thanks to BUET for providing me necessary funds.

Finally, I would like to express a very special indebtedness to my parents and wife whose encouragement and support was a continuous source of inspiration for this work.

ABSTRACT

Constitutive modeling for engineering materials is a great concern for the numerical modeling of engineering structures. In the last four decades, the constitutive modeling has evolved considerably. Starting from pioneering work by Druker and Prager [1952], various improvements, extensions and alternative constitutive models have been proposed. As materials often are subjected to repetitive loading during their service load such as wind load, earthquake load, moving traffic load etc. it is very essential for a complete model to simulate the cyclic behavior of the material accurately like the monotonic one. In this regard, several cyclic constitutive model have been proposed within the framework of the classical plasticity theory such as Prager [1956], Armstrong and Frederick [1966], Mróz [1967], Dafaslias and Popov [1975, 1976], Chaboche and his coworkers [1979, 1986], Ohno and Wang [1993], Hossain, Siddiquee and Tatsuoka [2005] etc. All of these models have the ability to simulate the cyclic stress-strain behavior of various materials with some limitations of their own. In this research work an attempt is made to develop a robust cyclic constitutive model within the framework of the theory of plasticity.

To construct a generalized constitutive model for both the pressure independent and dependent materials, a general framework for the cyclic modeling has been proposed. In this framework a nonlinear kinematic hardening rule is derived from the concept of the instantaneous slope of the stress-strain relationship. For this purpose a proportional rule and a drag rule is formulated. By using the proportional rule, the modified Masing's rule is fulfilled which has been observed for many materials. Using the drag rule, the overshooting or the undershooting of the stress-strain relationship can be modeled.

A nonlinear stress-strain relationship is indispensable to develop a constitutive model. Often a simple hyperbolic equation (Konder, R.L. [1963]) is used. In the present research a nonlinear stress-strain relationship is proposed which is simple but fulfills all the necessary requirements. Using this equation the instantaneous slope is calculated. By using this instantaneous slope for kinematic hardening rule, models for both the pressure independent and dependent materials

have been developed. The Von-Mises and Druker-Prager yield functions are used for pressure independent and pressure dependent materials respectively. Then an associative flow rule is adopted for the pressure independent material and a stress-dilatancy rule proposed by Tatsuoka et. al. [2003] is used with some modification for pressure dependent material.

For the integration of the of the incremental stress-strain relationships, several integration algorithms are available. In the present work, Return Mapping algorithm is used (Ortiz and Popov [1985], Simo and Taylor [1986] and Ortiz and Simo [1986]). Finally, for the nonlinear solution of the finite element analysis Dynamic Relaxation technique is used.

To verify the model, a single four node quadrilateral element is chosen with single gauss point integration for plane strain simulation. Masuda et. al. [1999] performed a series of plane strain cyclic loading tests on Toyoura sand. In this research, an attempt is made to simulate the cyclic plane strain behavior of Toyoura sand and the results have been found quite reasonable. The proposed model can be applicable for any type of structural as well as soil-structure interaction problems.

CHAPTER 1

INTRODUCTION

1.1 General

Mathematical modeling of the behavior of materials has been thriving at the goal of simulating a wide range of materials under various loading, boundary conditions for the last four decades. Materials are often subjected to transient and cyclic stresses due to earthquake or other source of dynamic load. Many models have been introduced to simulate the cyclic stress-strain behavior of materials like steel, reinforced concrete, soil etc. such as Prager [1956], Armstrong and Frederick [1966], Mróz [1967], Dafalias and Popov [1975,1976], Ohno and Wang [1993], Hossain, [2005], Hossain, Siddiquee and Tatsuoka [2005] etc. These cyclic evaluations of the material are modeled through kinematic hardening, isotropic hardening and/or a combination of both. The kinematic hardening models are, again can be classified into two broad categories as coupled models or uncoupled models according to the dependence of their plastic modulus on kinematic hardening (Bari. [2001]). The cyclic evaluations of materials often resemble the features of extended Masing behavior. Masing's rule([Tatsuoka, Masuda, Siddiquee, and Koseki [2003], Montáns [2000]) states that the unloading curve keeps a homological ratio of two to monotonic one. It has been experimentally observed that this rule holds closely in most materials. The extension of this rule, also observed in most materials, is that the modelings process takes place through the initial monotonic curve or through previous reloading ones when they are intersected. The numerical simulation of this rule from isotropic and/or kinematic hardening requires difficult-to-obtain variable combinations of both hardening types. As isotropic hardening is mostly used for monotonic loadings, in the proposed research work kinematic hardening is used to simulate the cyclic behavior.

1.2 Research Motivation

In Prager's kinematic hardening model [1956], the incremental stress has a linear relationship with the plastic strain increment and as a result, a constant plastic flow occurs due to stress increment. So, this model gives a linear closed hysteresis stress strain behavior due to cyclic loading.

Mróz's model [1967] makes use of several nested yield surfaces that normally harden kinematically according to Mróz's rule in order to avoid mutual overlapping. Once the yield surface is reached, it is dragged by stresses until it contacts the next one. Then, the outer surface is also towed away until unloading occurs. In the meantime, a linear hardening is usually employed for proceeding loading. The more yield surfaces are used, the better the monotonic curve and the corresponding cycles are represented. This model, by construction, ensures Masing's rule. The loops are closed and stabilized after the first cycle and the monotonic curve is recovered once the previous threshold is surpassed. These are sometimes desirable attributes not only from a physical point of view but also from a computational standpoint. But the model has its drawbacks. The first one is that if one wishes to accurately represent the evaluation of the material for both small and relatively large strains and for both monotonic and large loading many surfaces are needed. This implies the need of large memory, since it is essential to save the positions of each of one of those surfaces. It is also required many checks to keep track of which surfaces become active and which ones become inactive, and many operations to move the back-stress-tensor of each surface.

To overcome these computational inconveniences, researchers developed bounding surface models. The bounding surface models are based on the idea of Dafalias and Popov [1975] of utilizing an admissible domain for the stresses and computing the hardening function from the distance of stress tensor to the bounding surface. Thus, the hardening function has the property of depending only on the stress-tensor during discrete load step. The hardening function of this kind of models has some interesting properties. It is a continuous function and performs cycles with smooth translation to a monotonic reloading curve somehow related to the original one. The formulation is not too difficult to implement and has second order convergence if an elastoplastic tangent consistent with the algorithm is used. The memory effect may also be included in a simple way. Nevertheless, bounding surface models have one important drawback. The cycle do not recover initial monotonic loading curve, they do not stabilize just after the first cycle and they do not fulfill Masing's rule. Although this behavior some times is closer to actual behavior of material, usually it is not. Furthermore, the relationship between the initial backbone curve and the unloading curve changes with the stress level. This fact has one additional computational inconvenience, it is difficult to obtain parameters of hardening function that are valid for all stress levels and all types of loading.

Armstrong and Frederick's [1966] hardening rule has a similar type of characteristics like the Bounding Surface model. But this type of model shows much ratcheting due to small cyclic loading and unloading and as the dynamic recovery term is proportional to the back-stress-tensor, it does not allow the hysteresis loop to close at all and they do not fulfill Masing's rule.

Ohno and Wang's [1993] model basically gives the same kind of result like the Mróz's model and the complexities of computation are reduced due to the threshold dynamic recovery term. But the memory requirement is more than the Bounding Surface model or Armstrong and Frederick's model due to the multiple surfaces. The main drawback is this model gives a piece wise linear closed hysteresis loops.

Hossain, Siddiquee and Tatsuoka's [2005] Model can well simulate the cyclic behavior of any pressure independent material. It gives a non-liner closed hysteresis stress-strain curve due to the cyclic loading. But the memory requirement and computatinal complexity is high.

In the present research work, there is effort to develop a model that overcomes all the above mentioned drawbacks. Structures are often subjected to cyclic loading coming from machine vibration, wind, earthquake etc. So, in the soil-structure interaction problems, finding the response of the two constituent materials under these dynamic loads is a difficult task. The structure may be single phase material like steel or two phase material like reinforced concrete and the soil is a three phase material. There are also various models to simulate the behavior of structural material like Drucker [1951], Chen [1982], Ahmad [2002] etc. and soil like Cam Clay Model (Schofield and Wroth [1968]), Vremeer [1978], Siddiquee [1994] etc. for monotonic loadings. However, a general robust plasticity model is required to model the materials under cyclic loadings.

1.3 Research Objectives

The objective of the present research is therefore to develop a general nonlinear equation to simulate the nonlinear stress-strain relationship of materials and to develop a method to simulate the cyclic stress-strain relation of both pressure dependent materials like sand etc. and pressure independent materials like reinforced concrete, steel, cay etc. subjected to irregular cyclic loading history. Thus, the model developed has the advantage of a direct relevance to Masing's rule and the cycle is closed and the monotonic curve is recovered after the previous threshold has been surpassed. Also, there are efforts to reduce the computational cost substantially from that of traditional multi-surface models.

Furthermore, the proposed model is validated through a single element finite element analysis with various experimental results form the literature such as Tatsuoka, Masuda, Siddiquee, and Koseki [2003].

1.4 Methodology

To develop a general nonlinear equation to simulate the nonlinear stress-strain relationship of materials a simple nonlinear stress-strain equation is proposed. Then, using this equation as the backbone curve for finding the instantaneous slopes of Prager's kinematic hardening rule, a kinematic hardening model is developed. As we know Prager's model follows a linear kinematic hardening rule corresponding to translation of the loading surface. Here, a model is developed which follows the Prager's kinematic hardening rule with the modification that the slope of the stress-strain curve is changed with the instantaneous slope of the nonlinear stress-strain equation. Thus a nonlinear stress-strain relationship is found unlike that from Prager's model. Then by following the extended Masing's Rule the cyclic bevavior of the materials is simulated in such a way that the cycle is closed one and the monotonic curve is recovered after the previous threshold has been surpassed. To simulate the stress-dilatancy relationship, a stress-dilatancy relationship proposed by Tatsuoka, Masuda, Siddiquee, and Koseki [2003] is used with some modification. Then for the non-linear solution of FE, the Dynamic Relaxation [DR] (Underwood [1983]) method is applied and return mapping algorithm (Ortiz and Simo [1986]) is applied for the integration of incremental stress-strain relationships. The model is validated with the experimental results such as with the results of Tatsuoka, Masuda, Siddiquee, and Koseki [2003] with a single element test. In this stage, appropriate parameters of the model is evaluated.

1.5 Organization of the Thesis

The thesis consists of nine chapters including the present one. The first chapter deals with the introduction, research motivation, scope & objectives and methodology. Chapter two reviews the related literatures about the plasticity theory, constitutive models of materials for cyclic loading, integration algorithm, finite element method and solution techniques. Chapter three describes a noble kinematic hardening rule for cyclic plasticity. Chapter four describes the formulation of models for pressure independent and pressure dependent materials. Chapter five describes the integration algorithm for the cyclic plasticity models. Chapter six discusses the solution technique of the nonlinear finite element method. Chapter seven describes the simulated results and model validation for the cyclic plane strain response. Summary, conclusions and future research scope are presented in chapter eight.

CHAPTER 2
LITERATURE REVIEW

2.1 Introduction

In this literature review, the development of mathematical models for materials subjected to cyclic loading has been discussed. These models are based on the concept of hardening plasticity where isotropic hardening, kinematic hardening rule or mixed hardening rule has been applied. This review is divided in five parts consisting of description of the plasticity theory, constitutive models of materials for cyclic loading, integration algorithm, finite element method and solution techniques.

2.2 Plasticity theory

The theory of Plasticity involves the calculation of permanent deformation of materials. Moreover, the Plasticity models are based three fundamental assumptions:

- The shape of an initial yield surface.
- The evolution of subsequent loading surface (Hardening rule).
- The formulation of an appropriate flow rule.

Inside the initial yield surface, the region is called elastic region. Loading beyond this elastic region causes permanent deformation known as plastic deformation. The rate of the plastic deformation is defined by a hardening rule and by using this hardening rule, the evolution of subsequent loading surface is defined. The flow rule defines the direction of the plastic strain increment for each incrimination of the load.

Again, the endocroic plasticity, proposed by Valanis (1971), is based on continuous model for elastoplastic behaviour and it does not require the existence of yield surface. In this theory, the constitutive equation is integral or differential form based on a pseudo time scale, the intrinsic time.

2.2.1 Hardening rule

Hardening process can basically be attained in two parametric ways:

- Plastic work (in work hardening models)
- Plastic strain (in strain hardening models)

There are several hardening rules. The choice of a particular one depends on its ability to represent the hardening behavior of a particular material. Generally, there are three types of hardening:

a. Isotropic hardening.
b. Kinematic hardening
c. Mixed hardening.

2.2.1.1 Isotropic hardening

The simplest isotropic hardening model assumes that the yield surface expands uniformly from the hydrostatic axis without distortion, depending upon plastic strain/work history. So, the equation of the subsequent yield surface or loading surface can be written as:

$$F(\sigma_{ij}) = k^2(\varepsilon_p) \qquad 2.1$$

Where, ε_p = the effective plastic strain. Usually it is the integrated function of plastic strain components. This kind of hardening is good for isotropic material behavior.

2.2.1.2 Kinematic hardening

This kind of hardening assumes that loading surface translates as a rigid body in the stress space during plastic deformation. In order to simulate anisotropic behavior this kind of hardening is very effective. Mathematically:

$$f(\sigma_{ij}, \varepsilon_{ij}^p) = F(\sigma_{ij} - \alpha_{ij}) - k^2 = 0 \qquad 2.2$$

Where, k is the material strength constant. α_{ij} are the coordinates of the center of the loading surface which changes with plastic flow. Multi surface model proposed by Mróz and bounding surface model proposed by Dafalias use this kind of hardening.

2.2.1.3 Mixed hardening

A combination of previous two hardening models leads to a more realistic mixed hardening model, which can predict different degree of the Bouschinger effect.

2.2.2 Flow rule

Only the normal stress component produces the plastic strain increment, which is also proportional to this stress increment. So,

$$d\varepsilon_{ij}^{p} = d\lambda \frac{\partial \phi}{\partial \sigma_{ij}} \qquad 2.3$$

Where, $d\lambda = \frac{1}{H'}(\frac{\partial f}{\partial \sigma_{ij}} d\sigma_{mn})$

Here H' is the hardening modulus, which generally depends on stress, strain and history of loading and ϕ is the plastic potential function.

2.3 Frameworks for Cyclic Plasticity

The modeling of cyclic plasticity responses is quite complex. Many models have been introduced to simulate the cyclic stress-strain behavior. These cyclic evaluations of the material are modeled through kinematic hardening, isotropic hardening and/or a combination of both. The kinematic hardening models are also can be classified into two broad categories as coupled models or uncoupled models according to the dependence of their plastic modulus on kinematic hardening (Bari. S. [2001]). A review of several coupled and uncoupled models are given below.

2.3.1 Coupled Models

In the coupled modeling scheme, the plastic modulus calculation is coupled with the kinematic hardening rule through the consistency condition of the yield surface. The coupled models can be categorized according to their hardening features such as linear kinematic hardening model (Prager [1956]), nonlinear kinematic hardening model (Armstrong and Frederick [1966]), decomposed nonlinear kinematic hardening model (Chaboche and his coworkers [1979, 1986]), decomposed nonlinear kinematic hardening model with threshold (Chaboche [1991], Ohno and Wang [1993], Ohno and Abdel Karim [2000], Chen and Jiao [2004]) and isotropic hardening with origin shift (Hossain, Siddiquee and Tatsuoka [2005]). A brief review of some of these models are given as follows.

2.3.1.1 Prager's Kinematic Hardening Model

Prager's model follows a linear kinematic hardening rule. The kinematic hardening corresponds to translation of the loading surface. Mathematically,

$$f(\sigma_{ij}, \varepsilon_{ij}^{p}) = F(\sigma_{ij} - X_{ij}) - k = 0 \qquad 2.4$$

Where X_{ij} are the coordinates of the center of the loading surface which changes with the plastic flow. And the Prager's kinematic hardening rule is as follows

$$dX_{ij} = Cd\varepsilon_{ij}^{p} \qquad 2.5$$

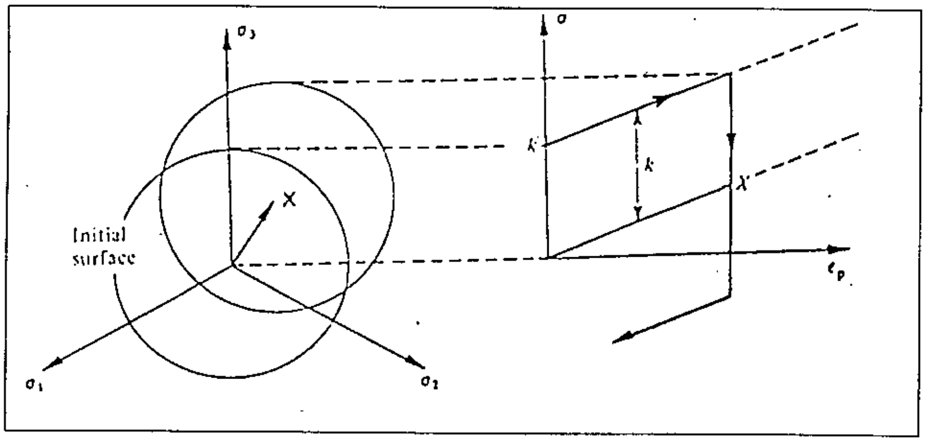

Figure 2.1: Prager's Hardening Rule (Lemaitre and Chaboche [1990])

In Prager's kinematic hardening model, the incremental stress has a linear relationship with the plastic strain increment and as a result, a constant plastic flow occurs due to stress increment. Therefore, this model gives a linear closed hysteresis stress strain behavior due to cyclic loading.

2.3.1.2 Armstrong and Frederick's Model

Due to the inconvenience of Prager's rule to give a nonlinear hysteresis relationship, Armstrong and Frederick introduced a fading memory effect of the strain path as a recovery term. So the resulting kinematic hardening rule has become as follows,

$$d\alpha_{ij} = \frac{2}{3}Cd\varepsilon_{ij}^{p} - \gamma\alpha_{ij}dp \qquad 2.6$$

Where in the increment of the accumulative plastic strain. Chaboche and his coworkers [1979, 1986] have decomposed this kinematic hardening rule into M components as follows

$$\alpha_{ij} = \sum_{k=1}^{M} (\alpha_{ij})_k \qquad 2.7$$

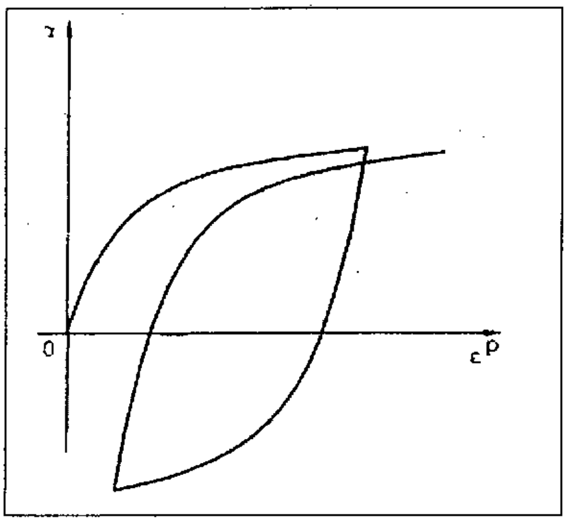

Figure 2.2: Change of α_i under loading, unloading, reverse loading, and reloading (Ohno and Wang [1993])

Armstrong and Frederick's hardening rule has a similar type of characteristics like the Bounding Surface model. However, this type of model shows much ratcheting due to small cyclic loading and unloading and as the dynamic recovery term is proportional to α_{ij}, it does not allow the hysteresis loop to close at all and they do not fulfill Masing's rule.

2.3.1.3 Ohno and Wang's Model

Ohno and Wang modified the Chaboche's model by assuming that the dynamic recovery of α_i is activated fully only when its magnitude $\bar{\alpha}_i$ attains a critical value, resulting from the energy required for cross slip. The critical state of dynamic recovery is represented by a surface

$$f_i = \overline{\alpha_i^2} - r_i^2 = 0 \tag{2.8}$$

Now with the Heaviside step function H, then, an evolution equation of α_i has been written in the following form in which the dynamic recovery term operates only when $\overline{\alpha}_i = r_i$:

$$\dot{\alpha}_i = \frac{2}{3} h_i \dot{\varepsilon}^p - H(f_i)\dot{\lambda}_i \frac{\alpha_i}{r_i} \tag{2.9}$$

The unknown parameter in this equation, $\dot{\lambda}_i$, is determined using the condition $\dot{f}_i = 0$, representing that α_i remains in the critical state $f_i = 0$ if currently $f_i = 0$ and $\dot{\varepsilon}^p : \alpha_i \geq 0$ (Figure 2.3):

$$\dot{\lambda}_i = h_i < \dot{\varepsilon}^p : k_i > \tag{2.10}$$

where k_i denotes the direction of α_i.

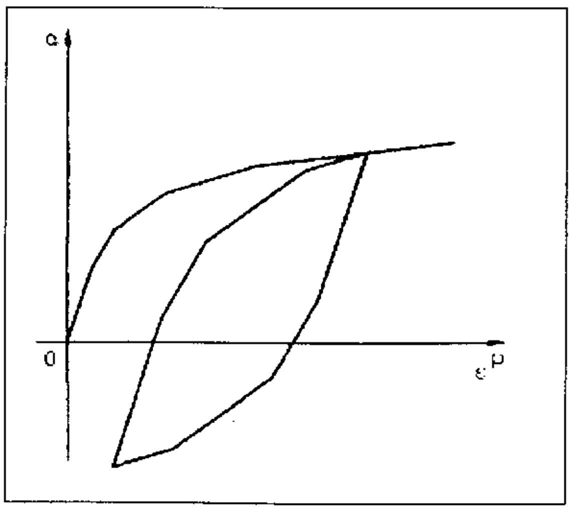

Figure 2.3: Change of α_i under loading, unloading, reverse loading, and reloading (Ohno and Wang [1993])

Ohno and Wang's model gives the same kind of result like the Mróz's model and the complexity of computation is reduced due to the threshold dynamic recovery term. But the memory requirement is more than the Bounding Surface model or Armstrong and Frederick's model due to the multiple surfaces. The main drawback is this model gives a piece wise linear closed hysteresis loops.

2.3.1.4 Hossain, Siddiquee and Tatsuoka's Model

In this model an isotropic strain hardening single surface model is formulated within a new framework to simulate the cyclic behavior of material. Hardening part of the model is achieved through a hyperbolic equation, which can model the non-linear stress-strain relationship. The cyclic behavior is simulated by introducing a frame work in which the origin of the stress-strain space is shifted to the instantaneous stress point while the direction of the loading is reversed. Then the yield surface again grows isotropically from the new origin.

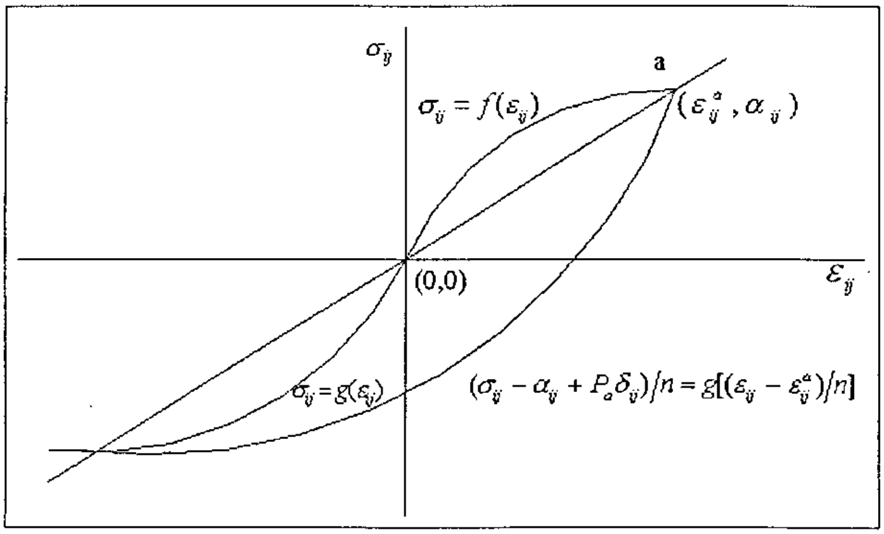

Figure 2.4: Framework for cyclic loading (Hossain, Siddiquee and Tatsuoka [2005])

Here during loading the stress state moves from the origin to the Point a where $\sigma_{ij} = \alpha_{ij}$ for a corresponding strain $\varepsilon_{ij}^{\alpha}$ following a loading curve $\sigma_{ij} = f(\varepsilon_{ij})$. Now when the unloading starts the origin is shifted to α_{ij} and the direction of the stress tensor σ_{ij} and strain tensor ε_{ij} is reversed. Now all the calculation is made from the new origin and yield surface grows isotropically from it. And the unloading curve follows the equation

$(\sigma_{ij} - \alpha_{ij} + P_a\delta_{ij})/n = g[(\varepsilon_{ij} - \varepsilon_{ij}^a)/n]$ where n is ratio between unloading curve to the unloading skeleton curve. It is obtained by using a proportionality rule where a straight line is drawn from the point of stress reversal passing the origin O to intersect the unloading skeleton curve and thus finds the value of n. If the loading and unloading skeleton curves are similar in shape, n is equal to two, which is stated by Masing's rule.

If the confining pressure at O is P_0 and at Point a it is $P_0 + \Delta P$, then set P_a as $P_0 - \Delta P$. This confining pressure ensures a smooth connection between the unloading curve and the unloading skeleton curve.

When the unloading curve intersects the unloading skeleton curve, origin is restored to the original position and the stress-strain relationship is found by the hyperbolic relationship of $\sigma_{ij} = g(\varepsilon_{ij})$. Thus a close hysteretic stress-strain relation is found giving the most accurate material response. Now by employing the drag rule we can simulate the increase in stress amplitude for same strain value during cyclic loading.

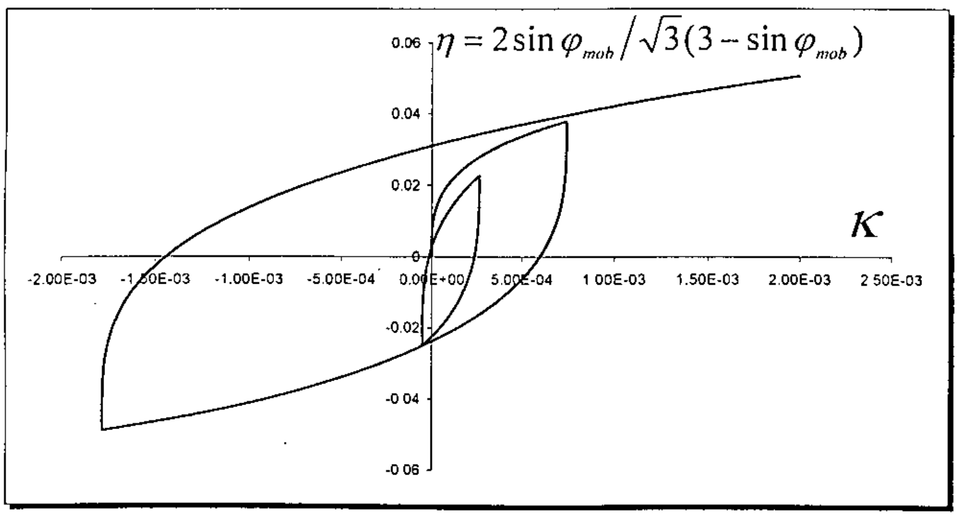

Figure 2.5: $\eta \sim \kappa$ Curve (Hossain, Siddiquee and Tatsuoka [2005])

This model can well simulate the cyclic behavior of any pressure independent material. It gives a non-liner closed hysteresis stress-strain curve due to the cyclic loading. However, the memory requirement and computatinal complexity is high for this model.

2.3.2 Uncoupled Models

In the uncoupled modeling scheme, on the other hand, the plastic modulus may be indirectly influenced by the kinematic hardening rule but its calculation does not depend on it. Following the pioneering work of Mróz [1967] new concept of uncoupled models have been introduce as multi-surface models (Ohno and Wang [1991], Khoei and Jamali [2004]) and as two-surface models (Dafaslias and Popov [1975, 1976], Hashiguchi [1980], Hashiguchi and Chen [1998], Montans [2000],). A brief review of some of these models are given as follows.

2.3.2.1 Mróz's Multisurface Model

Instead of using a single yield surface in stress space, Mróz [1967] postulated a family of yield surfaces with each surface translating independently in a pure kinematic manner, or individually obeying a linear work hardening model. This combined action, in general gives rise to a multilinear work hardening behavior for the material as a whole.

The mathematical forms of multi-surfaces $f_0, f_1, ..., f_m, ..., f_p$ with respective sizes $k^{(0)} < k^{(1)} < .... < k^{(m)} < .... < k^{(p)}$ are defined by:

$$f_m = f_m[\sigma_{ij} - \alpha_{ij}^{(m)}, k^{(m)}] = 0 \quad (m = 0, ..., p) \qquad 2.11$$

Where $\alpha_{ij}^{(m)}$ are the coordinates of center of yield surface in stress space and $k^{(m)}$ is its current size. $\alpha_{ij}^{(m)}$ and $k^{(m)}$ are, under a certain conditions, assumed to be functions of plastic strain, ε_{ij}^{p}.

Assuming now the translation of yield surface, f_m, denoted by the translation rule,

$$d\alpha_{ij}^{(m)} = d\mu \frac{k^{(m+1)} - k^{(m)}}{k^{(m)}} [\sigma_{ij}^{(m)} - \alpha_{ij}^{(m)}] \qquad 2.12$$

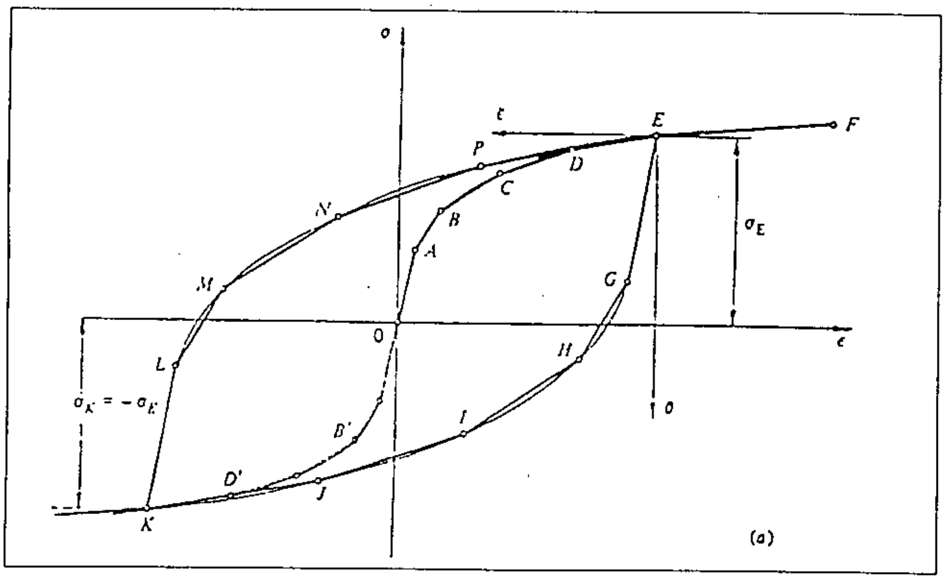

Figure 2.6: Behavior of Mróz's model (Lemaitre and Chaboche [1990])

This model, by construction, ensures Masing's rule. The loops are closed and stabilized after the first cycle and the monotonic curve is recovered once the previous threshold is surpassed. These are sometimes desirable attributes not only from a physical point of view but also from a computational standpoint. Nevertheless, the model has its drawbacks. The first one is that if one wishes to accurately represent the evaluation of the material for both small and relatively large strains and for both monotonic and large loading many surfaces are needed. This implies the need of large memory, since it is essential to save the positions of each of one of those surfaces. It is also required many checks to keep track of which surfaces become active and which ones become inactive, and many operations to move the back-stress-tensor of each surface. In addition, the stress-strain relationship found in this model is piecewise linear one.

2.3.2.2 Bounding Surface Model

Dafalias and Popov [1975] have propose an alternative, but conceptually similar model to that by Mróz, for kinematic and isotropic hardening. Instead of defining a series of surfaces, individually, two surfaces, a bounding or limiting surface and a loading surface are defined. The loading surface is defined as:

$$f(\sigma_{ij} - \alpha_{ij}, q_n) = 0 \qquad 2.13$$

Where, α_{ij} are the centers of coordinates of the loading surface and q_n are the plastic internal variables such as the plastic strain. The loading surface is allowed to translate as well as to deform under any hardening rule assumed appropriately, and it may contact the bounding surface, but not intersect it. With in the framework of associated flow rule assumption, the generalized hardening modulus H' related to the loading surface is given by:

$$H' = H'(\delta, w_p) \qquad 2.14$$

Where the δ is the distance between the current stress state σ_{ij} represented as point a on the loading surface and the stress state $\overline{\sigma_{ij}}$ at the point b which is obtained by the intersection of the line $\overline{ka}$ with the bounding surface and w_p is the plastic work which is integrated in the plastic strain space along the loading path during the plastic deformation prior to the elastic deformation preceding the current plastic state. Plastic hardening modulus on the loading surface is assumed to very depending on the relative configuration of the loading and bounding surface.

On the other hand, the bounding surface is defined as the homogeneous function of the form:

$$F(\sigma_{ij} - \alpha^{\bullet}_{ij}, q_n) = 0 \qquad 2.15$$

Where $\alpha^{\bullet}_{ij}$ are the center coordinates of point r for the bounding surface. The bounding surface translates in the stress space following the rule given by:

$$d\alpha^{\bullet}_{ij} = \frac{d\sigma}{\cos\omega} v_{ij} - \left(1 - \frac{H'_0}{H'}\right) d\sigma \mu_{ij} \qquad 2.16$$

Where $d\alpha^{*}_{ij}$ is the increment of the center translation of the bounding surface, $(d\sigma/_{\cos\omega})v_{ij}$ represents the increment of point a in the direction of the unit vector v_{ij} due to the translation of the loading surface. H'_0, Hardening modulus of contact with $\delta = 0$, $d\sigma$ the projection of $d\sigma_{ij}$ onto the normal vector n_{ij} at point a, and μ_{ij} the unit vector along points a and c at which the normal vectors are identical.

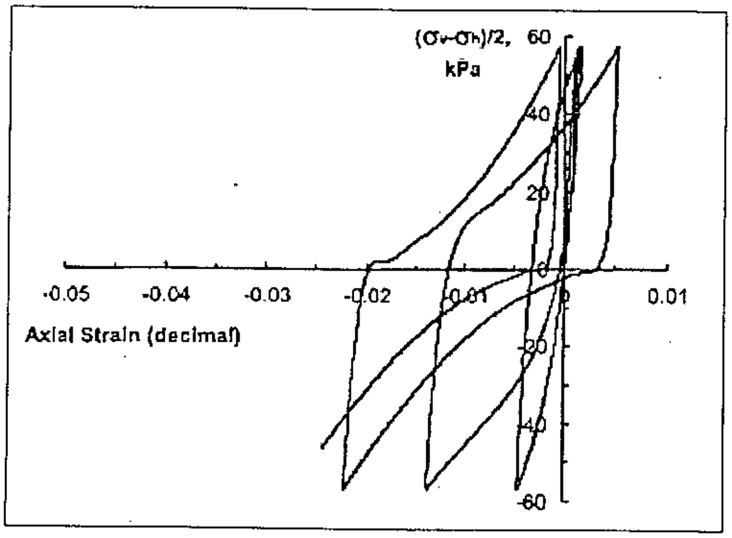

Figure 2.7: Model Simulation (Dafalias and Manzari [2004])

In this model, the hardening function has the property of depending only on the stress-tensor during discrete load step. It is a continuous function and performs cycles with smooth translation to a monotonic reloading curve somehow related to the original one. The formulation is not too difficult to implement and has second order convergence if an elastoplastic tangent consistent with the algorithm is used. The memory effect may also be included in a simple way. Nevertheless, bounding surface models have one important drawback. The cycle do not recover initial monotonic loading curve, they do not stabilize just after the first cycle and they do not fulfill Masing's rule. Although this behavior some times is closer to actual behavior of material, usually it is not. Furthermore, the relationship between the initial backbone curve and the unloading curve changes with the stress level. This fact has one additional computational inconvenience, it is difficult to obtain parameters of hardening function that are valid for all stress levels and all types of loading.

2.3.2.3 Subloading Surface Model

Early versions of the subloading surface model, e.g. Hashiguchi [1980], were quite similar to the bounding surface model. In the Extended subloading surface (Hashiguchi and Chen [1998]) isotropic hardening, translational and rotational kinematic hardening has been incorporated in a straightforward fashion. The normal yield surface $\hat{f}$ is defined:

$$\hat{f} = \hat{J} - F = 0 \qquad 2.17$$

in which $\hat{J}$ is a stress intensity that specifies the shape of the yield surface, F is an isotropic internal variable that determines the size of the yield surface, and a ˆ is used to refer to the yield state.

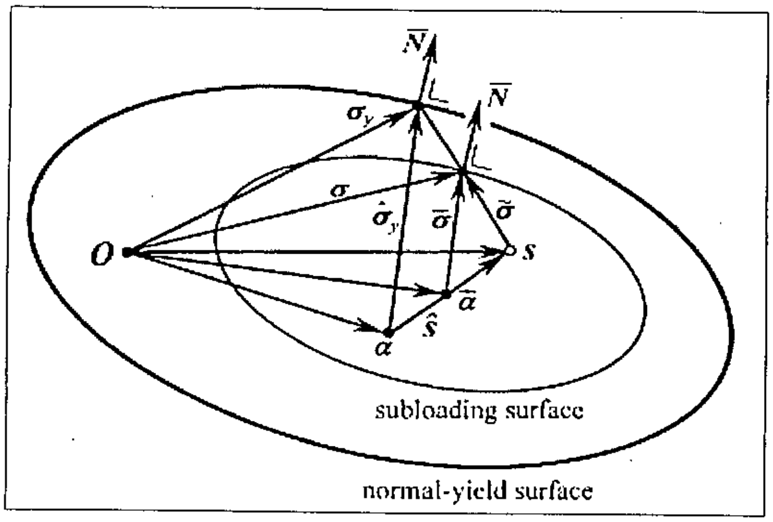

Figure 2.8: The normal yield and subloading surface (Hashiguchi and Tsutsumi [2001])

Inside the yield surface there exists a subloading surface $\bar{f}$ which can expand, shrink, translate and rotate as follows

$$\bar{f} = \bar{J} - RF = 0 \qquad 2.18$$

here, the bar refers to quantities on the subloading surface, measured with respect to the origin of the subloading surface, α. Thus, $\bar{J}$ is determined similar to $\hat{J}$, but with

$$\overline{\sigma} = \sigma - \alpha \qquad 2.19$$

where by definitionα follows from

$$\alpha = (1 - R)S \qquad 2.20$$

Where R is an internal parameter to scale the isotropic hardening variable F, i.e. the size of the yield surface S is the similarity center that always moves along the line joining the conjugate stress $\hat{\sigma}$ and the current stress σ.

2.3.2.4 Khoei and Jamali's Model

This model is of a von-Mises type with associated flow rule within multi-surface framework. The Mroz translation rule is implemented to the movements of the yield surfaces. The model is developed in the class of kinematic hardening models, so the 'Masing' rule is preserved. The model is able to consider the plastic strain accumulation in constant axial stress state, such as ratcheting. The implementation is validated by means of a simple deformation path of combined extension and compression test, a pure shear test with pseudo-random loading, a test which demonstrates the capabilities of the model in simulation of cyclic loading and ratcheting, a cyclic shear test in saturated undrained sand and finally, the analysis of a plate with holes, which presents the shear band using the multi-surface plasticity model.

2.4. Integration algorithm

The numerical solution of elastic-plastic boundary value problems is based on an iterative solution of the discretized momentum balance equations. Typically, for every load/time step, solution involves the following steps: Give a converged configuration at step n:

1. The discretized momentum equations are used to compute a new configuration for step (n+1) via an incremental motion which is used to compute at every stress point incremental strains $\Delta\varepsilon$;
2. At every stress point, for the given incremental strains $\Delta\varepsilon$, new values of the state variables (σ_{n+1}, S_{n+1}) and ε^{p}_{n+1} are obtained by integration of the local constitutive equations;

3. From the new computed stresses, balance of momentum is checked and if violated iterations are performed by returning to step 1.

For relatively simple models, it is possible to obtain an analytical solution of differential equation that relates the stress rate to strain rate, but for more complicated models, numerical techniques must be employed. Although radial return methods (Wilkins [1964], Kreig and Kreig [1977]) and sub-incrementation techniques (Nayak and Zienkiewicz [1972]) have been proposed in early days, no firm algorithmic basis was available until the pioneering work of Ortiz and Popov [1985], Simo and Taylor [1986] and Ortiz and Simo (1986). These semi-explicit algorithms are simple and efficient enough.

2.5. Finite element method

This is a robust method of solution to boundary value problems, which can accommodate high non-linearity of stress-strain relations of materials in the process of solution. Usually it satisfies all the requirements for an exact solution asymptotically, that means as the number of elements are increasing, the solution is also proceeding to an exact one. The finite element method (FEM) basically idealizes a continuum to discrete finite elements, where the shape and size need not be regular. This allows a convenient idealization of any metrical configuration with complex boundaries.

The method was first introduced by Turner, Clough, Martin and Topp [1956] and they used it for the analysis of airframes. Later on the main centers of developments were Swansea (Zienkiewicz et. al.), Stuttgart (Argyris and his co-workers) and the MIT. One of the most important features of FEM is that it depicts a complete picture of stress, strain and deformation characteristics throughout the domain of interest.

2.6. Solution technique

History of nonlinear finite element analysis is not so long. Most finite element computer programs still use an incremental loading procedure combined with modified Newton-Raphson (m.N-R) iteration to dissipate the out of balance.

The m.N-R method differs from Newto-Raphson method in a way that the stiffness matrix is neither reformed nor refactorized at each iteration. The economies that gained in m.N-R are offset by degradation in the convergence characteristics particularly for the later iterations.

Recently there is a major development of Newton type solutions (i.e., Conjugate Newton, Secant Newton, Quasi Newton). Considering there huge storage requirement, speed and complexity in calculation, they are not well suited to the material non-linearity solution. For that DR is well suited for its compact storage, easiness in iterative calculations.

The terminology " Dynamic Relaxation (DR) " first appeared in the paper of otter [1965] and Day [1965] in the mid-1960's. DR started to be improved by Welsh [1967], Cassel et al.[1968] due to introduction of the idea of fictitious mass. Rushton [1968] applied this method to solve nonlinear problems. Around early 1970's DR literature expanded a lot. Underwood [1983] presented adaptive DR methods and Papadrakakis [1981] showed how to select DR iteration parameters automatically. Felippa [1986] showed the analogy between QN (Quasi-Newton) and two-step-integrated DR methods and inferred that DR offers a potential insight on parameter selection for the QN update family.

Still accuracy and efficiency of DR is dependent on size of loading steps and mesh size. Force level DR cannot get to post peak behavior. And displacement-control DR can get the post peak load-displacement curve, but is accurate only when using very small displacement increments.

Considering all these factors, a more general solution algorithm can be resorted. Path controlled solution, which has been advocated first by Riks [1979] and Wempner [1971] then Crisfield [1981] and Ramm et. al. [1981], showed that it could be used as a successful tool to solve nonlinear equations arising from material nonlinearity. In case of DR, similar path-following algorithm is formulated first by Siddiquee [1994] in case of material nonlinearity.

2.7 Summary

In this chapter, a brief description of the plasticity theory, constitutive models of materials for cyclic loading, integration algorithm, finite element method and solution techniques are given. The classical plasticity theory is based on three mathematical functions as yield function, hardening rule and flow rule. The yield function defines the initial elastic region and subsequent loading surfaces due to the plastic flow. Hardening rule and flow rule defines the amount of plastic flow and its direction. There are several constitutive models are proposed to simulate the cyclic behavior of the materials. Some of these models are coupled models as the plastic modulus calculation is coupled with the kinematic hardening rule through the consistency condition of the yield surface where as some models are uncoupled models as the plastic modulus may be indirectly influenced by the kinematic hardening rule but its calculation does not depend on it. To integrate the incremental stress-strain relationship of the constitutive model several algorithm exist. Among these algorithms, the return mapping algorithm is a simple but robust algorithm. Finally, to solve the finite element nonlinear equations a nonlinear solution technique is required. In this regard, the Dynamic Relaxation technique is a robust technique to solve the governing equation.

CHAPTER 3

A NOVEL KINEMATIC HARDENING RULE FOR CYCLIC PLASTICITY

3.1 Introduction

Mathematical modeling of materials was of great interest during the last century due to the invention of digital computer. As a result, several constitutive models were proposed by the researchers to simulate the response of materials under monotonic loading as well as cyclic loading under the general framework of Elasto-plasticity. In the last three decades, one of the main objectives was to develop a robust cyclic plasticity model to with considerable accuracy for the engineering purpose. Following the pioneer work of Prager [1956], kinematic hardening was the major integral part of the most of these cyclic plasticity models. The nonlinear kinematic hardening rule of Armstrong and Frederick [1966] was extensively used modified by Chaboche and his co-workers [1976, 1986, 1991]. Finally, Ohno and Wang [1993] proposed a noble framework to simulate the cyclic behavior. All of these models are coupled models as the plastic modulus calculation is coupled with the kinematic hardening rule through the consistency condition. Another framework, proposed by Mróz [1967], known as multisurface model, can also well simulate the cyclic response. In this new concept, a series of loading surfaces move with a linear kinematic hardening rule which give rise of a piecewise linear stress-strain relationship. To reduce the complexity of several loading surfaces, a simple but robust framework of two surfaces was proposed by Dafalias and Popov [1975, 1976] known as bounding surface model. Based on these frameworks several models were proposed such as Hashiguchi [1980], Ohno and Wang [1991], Hashiguchi and Chen [1998], Montans [2000], Ohno and Abdel Karim [2000], Chen and Jiao [2004], Khoei and Jamali [2004] etc.

To model the cyclic behavior of materials, Masing's rule has a greate importance, as the cyclic evaluation some times resembles this feature. The Masing's rule states that, the unloading curve keeps a homological ratio of two to monotonic one. The extension of this rule, also observed in most materials, is that the modeling process takes place through the initial monotonic curve or through previous reloading ones when they are intersected (Montáns [2000]). Among the above frameworks, Mróz's multisurface framework [1967] and Ohno and Wang [1993] model can well simulate the Masing's rule with piecewise closed stress-strain loops. Montáns [2000] proposed a model that has the ability to simulate the Masing's rule within the bounding surface framework. In addition, Hossain, Siddiquee and Tatsuoka [2005] proposed a mode within the framework of isotropic hardening with the origin sift for each load reversals. Both of these models have the ability to produce nonlinear closed hysteresis stress-strain loops.

In this chapter a noble kinematic hardening rule for cyclic plasticity is proposed, which can simulate a generalize modified Masing's rule with different loading and unloading skeleton curves (Tatsuoka, Masuda, Siddiquee and Koseki [2003]). Here, the Prager's linear kinematic hardening rule is modified with a single parameter, which varies with the cumulative plastic strain.

3.2 Kinematic Hardening Rule

The kinematic hardening rule evolves with the accumulative plastic strain. Since the present model has been developed within the small strain range, the total strain increment can be decomposed into its elastic and plastic parts as follows,

$$d\varepsilon_{ij} = d\varepsilon_{ij}^{e} + d\varepsilon_{ij}^{p} \qquad 3.1$$

Where, $d\varepsilon_{ij}^{p}$ represents the incremental plastic strain. Now, the incrimination of the kinematic hardening variable α_{ij} can be given as,

$$d\alpha_{ij} = Cd\varepsilon_{ij}^{p} \qquad 3.2$$

Where, C is the instantaneous slope of the $\alpha_{ij} \sim \varepsilon_{ij}^{p}$ relationship. For a constant C the kinematic hardening rule reduces to Prager's linear kinematic hardening rule and results linear stress-strain curves.

In the proposed model, an evaluation rule for C is given as a function of the accumulative plastic strain. Firstly, the loading and unloading skeleton curves are scaled according to a modified Masing's rule upon the reversal of loading to get a closed hysteresis loop (Tatsuoka, Masuda, Siddiquee and Koseki [2003]). Then from the instantaneous slope of the curve, C is calculated as the model parameter. As a result a closed hysteresis relationship of $\alpha_{ij} \sim \varepsilon_{ij}^{p}$ is found. Thus, the model simulates nonlinear stress-strain relationship which obeys the modified Masing's rule.

3.2.1 Modified Masing's Rule

Tatsuoka et. al. [2003] modified the original Masing's rule to simulate the case of unsymetric loading and unloading skeleton stress-strain curves as well as the case where the unloading curve does not keep a homological ratio of two to monotonic one.

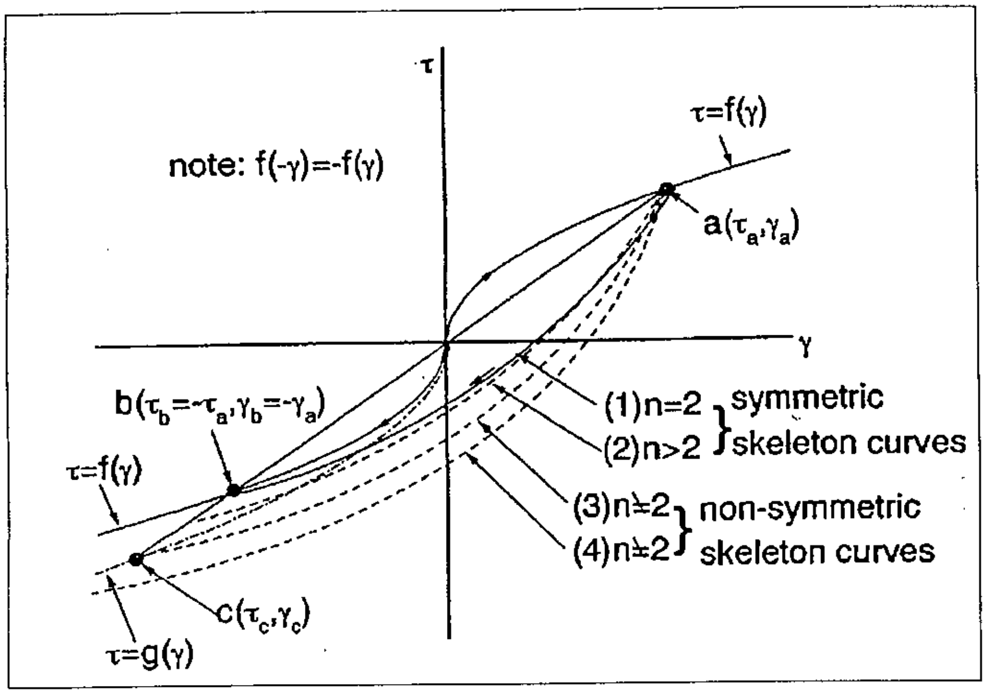

Figure 3.1: Schematic diagram explaining proportional rule (Masuda et al., 1999)

In Figure 3.1, $\tau = f(\gamma)$ represents the primary loading and unloading curves that are symmetric about the origin i.e., $f(-\gamma) = -f(\gamma)$. When the loading direction is reversed at Point a $(\tau_{a,}\gamma_{a})$, the unloading curve is given as

$$(\tau - \tau_a)/n = f[(\gamma - \gamma_a)/n] \qquad 3.3$$

Where n=2 (case 1). In this case, the unloading curve joins the unloading skeleton curve at the symmetric point b (τ_b, γ_b) with $\tau_b = -\tau_a$ and $\gamma_b = -\gamma_a$. On the other hand, many experimental results show that the unloading curve from point a does not join the skeleton curve at point b (case 2). In addition, the primary loading and unloading curves could be largely non-symmetric (case 3 and 4). In these cases, two different functions $\tau = f(\gamma)$ and $\tau = g(\gamma)$ should be assigned for loading and unloading curves. It could be assumed that the unloading curve from point a in this case is given as,

$$(\tau - \tau_a)/n = g[(\gamma - \gamma_a)/n] \qquad 3.4$$

For example, in case 3 we can find point c (τ_c, γ_c) = intersection of straight line passing the reversing point a and the origin and the unloading primary curve $\tau = g(\gamma)$. For unloading curve to join the primary unloading curve at point c, the factor n should be equal to $-(\tau - \tau_c)/\tau_c (\geq 0)$, which is usually different from two and may not be constant during cyclic loading. Therefore, the value of n can be determined by a proportional rule and a drag rule.

For the present model the relationship between η and the plastic hardening parameter κ is used to get the instantaneous slope C where, η is a model veriable and κ is the measure of accumulative plastic strain. For pressure independent materials, η has a direct relationship with the stress ratio R where, $R = \sigma_1/\sigma_3$ and for pressure dependent materials, η has a direct relationship with $\sin\varphi_{mob}$ where, $\sin\varphi_{mob} = (\sigma_1 - \sigma_3)/(\sigma_1 + \sigma_3)$.

3.2.2 Proportional Rule

Tatsuoka et. al. [2003] proposed a proportional rule to find the modified n for unsymmetric loading and unloading curves. The proportional rule consists of external and internal rules. Upon the reversal of loading direction, either external or internal rule is chosen for a given loading history based on the largeness of the current value of κ relative to instantaneous maximum and minimum value of κ as

κ_{max} and κ_{min}. To keep continuity between external rule and internal rule, it is assumed that a pair of points having coordinates κ_{max} and κ_{min} is always located on opposite side of the origin O on a straight line passing the origin. The meaning of κ_{min} and κ_{max} is explained below:

1. Suppose that loading starts from the origin and continue until Point A. At Point A, κ_{max} = the maximum value of κ ever achieved by loading = κ_A. Accordingly, κ_{max} at Point B (located along the first unloading curve from Point A) = κ_A. When the current κ value becomes larger than the previous value of κ_{max} (i.e., when $\kappa > \kappa_{max} = \kappa_A$), the previous value of κ_{max} is replaced by the instantaneous κ value.

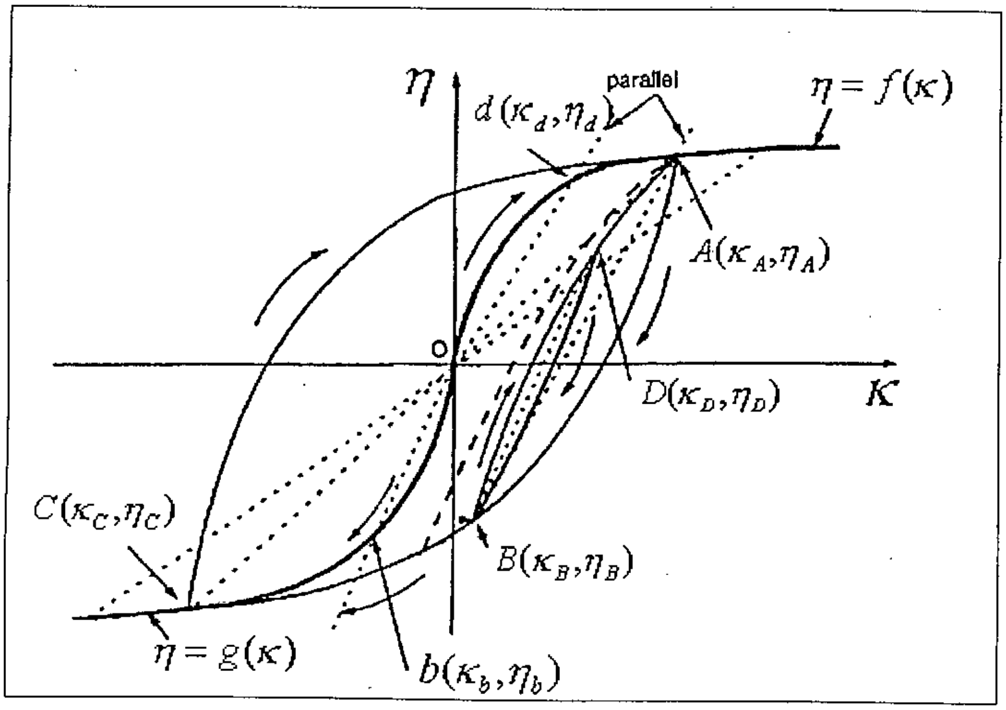

Figure 3.2: Details of proportional rule

2. The κ_{min} value is defined as the smaller value of (a) the smallest value of κ ever attained during unloading and (b) the κ value at the intersection of the straight line starting from the point of κ_{max} and passing the origin O with the

unloading skeleton curve $\eta = g(\kappa)$. The κ_{min} value of Point B = κ_C (κ at Point C), corresponding to Point A.

3. The κ_{max} value is defined as larger value of (a) the largest value of κ ever attained by loading and (b) the value of κ at the intersection of the straight line starting from the point of κ_{min} and passing the origin O with the loading skeleton curve $\eta = f(\kappa)$.

The rules to obtain the hysteretic relationship for cyclic loading are described below, referring to Figure 3.2 and 3.3:

1. Curves for reloading and so on are obtained as follows:
   - When unloading is reversed to reloading while renewing the κ_{min} value to the instantaneous plastic strain κ, the reloading curve is obtained by following external rule,
   - When unloading is reversed to reloading with $\kappa_{max} \geq \kappa \geq \kappa_{min}$ maintaining the previous κ_{max} and κ_{min}, the reloading curve is obtained by following the internal rule, and
   - When the loading is continued while renewing the κ_{max} value to instantaneous plastic strain κ, the loading curve $\eta = f(\kappa)$ is followed.

2. Curves for unloading and so on are obtained as follows:
   - When loading is reversed to unloading while renewing the κ_{max} value to the instantaneous plastic strain κ, the unloading curve is obtained by following external rule,
   - When loading is reversed to unloading with $\kappa_{max} \geq \kappa \geq \kappa_{min}$ maintaining the previous κ_{max} and κ_{min}, the unloading curve is obtained by following the internal rule, and
   - When the unloading is continued while renewing the κ_{min} value to instantaneous plastic strain κ, the unloading skeleton curve $\eta = g(\kappa)$ is followed.

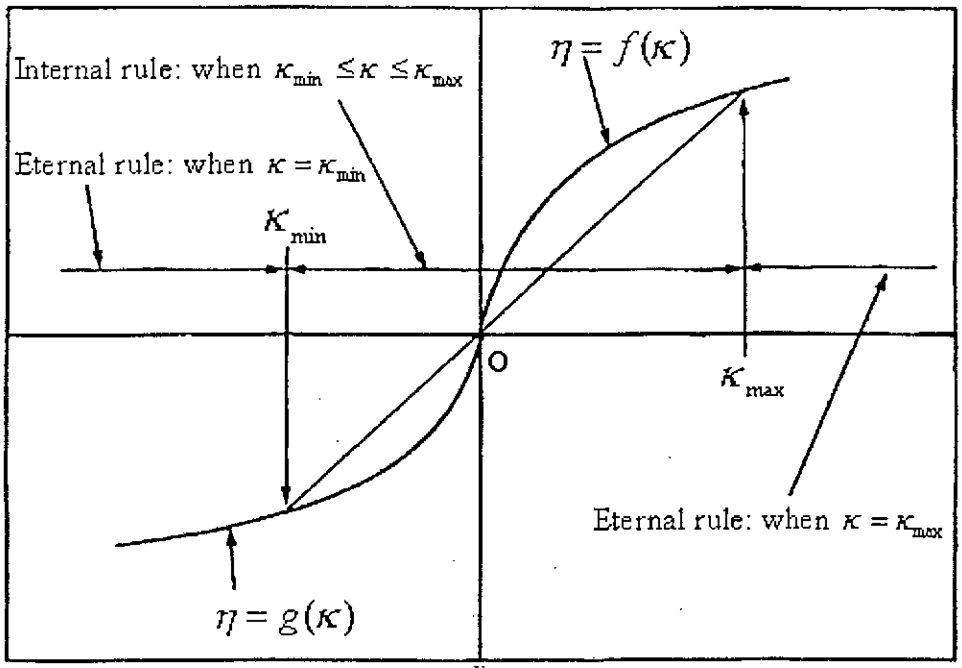

Figure 3.3: Rule to choose either external or internal rule for given instantaneous plastic strain κ

The rules are described below more specifically referring to Figure 3.2,

1. During the first primary loading from origin O (κ_0, η_0), where $\kappa_{max} = \kappa_{min} = 0$, until Point A, always $\kappa_{max} = \kappa$ and the curve follows the loading skeleton curve $\eta = f(\kappa)$. At Point A (κ_A, η_A), we have $\kappa_{max} = \kappa_A$ and $\kappa_{min} = \kappa_C$.
2. When loading is reversed at Point A, the unloading curve bound for Point C is obtained by following the external rule (with $\kappa_{max} = \kappa_A$) and using the known unloading skeleton curve $\eta = g(\kappa)$ and the coordinate at Point C (κ_C, η_C) as

$$\frac{\eta - \eta_A}{n_1} = g\left(\frac{\kappa - \kappa_A}{n_1}\right) \qquad 3.5(a)$$

$$n_1 = \frac{(-\eta_C) + \eta_A}{(-\eta_C)} = \frac{(-\kappa_C) + \kappa_A}{(-\kappa_C)} \quad (\geq 0) \qquad 3.5(b)$$

3. When unloading continues passing Point C, the curve follows the unloading skeleton curve $\eta = g(\kappa)$ with $\kappa_{\max}$ = instantaneous κ.

4. Here, the target plastic strain κ_{target} is introduced, which is defined the value of κ at that point for which the curve is bound after the loading direction is reversed. For unloading and reloading curves following the external rule, κ_{target} is equal to $\kappa_{\min}$ and $\kappa_{\max}$, respectively. In Figure 3.2 κ_{target} for the unloading curve starting from Point A bound for Point C is $\kappa_{\min} = \kappa_C$.

5. In Figure 3.2, when unloading is reversed to reloading at Point B, where κ is between $\kappa_{\min} = \kappa_C$ and $\kappa_{\max} = \kappa_A$, the reloading curve is obtained by following internal rule. The target point is assumed to be the same with the latest previous reversing point before Point B (i.e., Point A). Then, this reloading curve is obtained by scaling the loading skeleton curve as:

$$\frac{\eta - \eta_B}{n_2} = f\left(\frac{\kappa - \kappa_B}{n_2}\right) \qquad 3.6(a)$$

$$n_2 = \frac{\eta_A - \eta_B}{\eta_d} = \frac{\kappa_A - \kappa_B}{\kappa_d} \quad (\geq 0) \qquad 3.6(b)$$

Where Point d (κ_d, η_d) = intersection of the straight line starting from the origin O while parallel to the straight line between Points B and A with the loading skeleton curve $\eta = f(\kappa)$.

6. In Figure 3.2 when the loading direction is reversed at Point D, the re-unloading branch, which is bound for the latest previous point (i.e., Point B), is obtained by Equation 3.5(a), but using another scaling factor n_3 given below,

$$n_3 = \frac{(-\eta_C) + \eta_A}{(-\eta_C)} \frac{\eta_D - \eta_B}{\eta_A - \eta_B} = \frac{(-\kappa_C) + \kappa_A}{(-\kappa_C)} \frac{\kappa_D - \kappa_B}{\kappa_A - \kappa_B} \quad (\geq 0) \quad 3.7$$

At Point B, the re-unloading curve does not smoothly rejoin the previous unloading curve $A \to B \to C$. The unloading curve beyond Point B follows the curve $A \to B \to C$.

7. When following the internal rule, the κ_{target} value is always equal to the κ value at the latest previous reversing point (before the current reversing

point). For example, κ_{target} is $\kappa_A = \kappa_{\max}$ for the reloading branch $B \to A$ and κ_B for the re-unloading branch $D \to B$.

8. Whenever the previous reversing point is passed, all the memory of previous cyclic loading history is erased. So, the reloading curve beyond Point B is bound for Point A, not for Point D.

3.2.3 Drag Rule

Applying the proportional rule, the closed $\eta \sim \kappa$ relationship can be found that obeys the Masing's rule with unsymmetric loading and reloading curves. However, for some materials it was found that under cyclic loading, the closed loop relation does not holds. As a result, to simulate this, the kinematic hardening rule is modified as follows,

$$d\alpha_{ij} = (1+d)Cd\varepsilon_{ij}^{p} \qquad 3.8$$

Where, d is the drag parameter that accumulates for each reversal of load and is constant for a particular loading or unloading segment of curve. If the growth of d is positive then it results the over-shooting of the stress-strain curve due to reloading. And, if its growth is negative then it results the under-shooting of the stress-strain curve due to reloading.

3.3 Summary

In this chapter, a noble kinematic hardening rule is proposed. To formulate the rule, the Prager's kinematic hardening rule is modified by replacing the constant with an instantaneous slope of a nonlinear skeleton curve. The model has a direct relevance with the modified Masing's rule. The model has two rules as the proportional rule and the drag rule. The proportional rule describes how the skeleton curve will be scaled to get a closed loop relationship. Finally, the drag rule explains how the curves can be dragged to get the overshoot or undershoot material response.

CHAPTER 4

FORMULATION OF MODELS FOR PRESSURE INDEPENDENT AND PRESSURE DEPENDENT MATERIALS

4.1 Introduction

For the finite element analysis of materials under both monotonic as well as cyclic loading, a good constitutive model is indispensable. Starting from pioneering work by Druker and Prager [1952], various improvements, extensions and alternative plasticity theories have been proposed. For isotropic hardening, Von-Mises yield criteria, Tresca yield criteria with appropriate hardening rule are used for pressure independent materials where as for pressure dependent materials Druker-Prager yield criteria, Mohr-Coulomb yield criteria are more popular. In Cyclic plasticity, Elliptic loading and yield surfaces are more popular for two surface models. In addition, Von-Mises and Druker-Prager yield functions are used for pressure independent and pressure dependent materials respectively for their relative simplicity.

To evaluate the instantaneous slope *C*, a nonlinear $\eta \sim \kappa$ relationship is required. Often a simple hyperbolic equation (Konder, R.L. [1963]) is used to model the stress-strain relation. Also, many models have been introduced to simulate the nonlinear stress-strain relations such as Saenz [1964], Griffith, D.V. and Prevost, J.H. [1990], Tatsuoka et al [1993], Tanak, T., Al-Karni, A. and Alshenawy, A. [2006] etc. Some of these models cannot model the initial gradient of the stress-strain relations whereas some does not show a zero tangent at the peak strength state. Also, some model are only limited to the hardening part of the stress-strain relationship.

A mathematical model of nonlinear stress-strain relationship must satisfy several conditions like (i) the curve should have an initial gradient, (ii) it must go through the peak strength state, (iii) the corresponding gradient of the peak state must be zero, (iv) the curve should be all through continuous and differentiable, (v) a single function must be able to simulate both the pre-peak hardening part as well as post-peak softening part.

The simple hyperbolic function like Konder cannot predict the failure realistically though it can be forced to go through the particular point of peak strength. Beyond the peak strength, the stress continues to increase with increasing strain as the curve approaches to the failure condition asymptotically. A modified hyperbolic function is proposed by Griffith and Prevost that satisfies all the four criteria cited before. But it cannot predict the post-peak behavior and the parameters required for the function are complicated to calculate.

Tatsuoka et al proposed a nonlinear stress-strain relation called General Hyperbolic Equation (GHE), which can simulate the pre-peak stress strain behavior as well as post-peak strain softening relation with a smooth transition at the peak state. But the GHE has a complicated formulation, which requires a large number of parameters.

Takaka's model can simulate a series of stress strain curves with the limitation that it has a very stiff initially and it is not differentiable at zero strain. The model proposed by Al-Karni and Alshenawy has the ability to model both the hardening and softening part of the complete stress strain curve with an initial gradient. But the model also requires several material and calibrating parameters.

In this chapter, a simple nonlinear stress-strain model is proposed which can reasonably simulate a wide range of stress-strain relations for both hardening as well as softening parts. Then, by using this nonlinear relationship to evaluate $\eta \sim \kappa$ relationship, two pressure independent and pressure dependent models are developed based on the kinematic hardening framework proposed earlier with Von-Mises and Druker-Prager yield functions for pressure independent and pressure dependent materials respectively.

4.2 Modeling nonlinear stress-strain relations

The proposed model is an equation that relates the stress σ with the strain ε as follows,

$$\sigma = \sigma_p . \frac{\varepsilon_p + a}{\varepsilon_p^2} . \varepsilon . \left(\frac{\varepsilon_p + a}{\varepsilon + a} - \frac{a}{\varepsilon_p + a} \right) \text{ for hardening part} \qquad 4.1a$$

$$\sigma = \sigma_p . \frac{\varepsilon_p + m}{\varepsilon_p^2} . \varepsilon . \left(\frac{\varepsilon_p + m}{\varepsilon + m} - \frac{m}{\varepsilon_p + m} \right) \text{ for softening part} \qquad 4.1b$$

Where σ_p is the peak strength and the corresponding strain is ε_p and a is the material parameter which controls the shape of the curve. To find the value of a for the hardening part of the stress strain curve, equating the derivative of the curve at $\varepsilon = 0$ with the initial gradient E_0, we get,

$$\left(\frac{d\sigma}{d\varepsilon} \right)_0 = E_0 = \sigma_p . \frac{\varepsilon_p + a}{\varepsilon_p^2} . a . \left(\frac{\varepsilon_p + a}{a^2} - \frac{1}{\varepsilon_p + a} \right) \qquad 4.2$$

Also from the model and its derivative we can see that it satisfies the first four criteria cited before.

To model the post-peak behavior, we can find the value of m by equating the equation of the curve at $\varepsilon = \varepsilon_r$ and $\sigma = \sigma_r$ we get,

$$\sigma_r = \sigma_p . \frac{\varepsilon_p + m}{\varepsilon_p^2} . \varepsilon_r . \left(\frac{\varepsilon_p + m}{\varepsilon_r + m} - \frac{m}{\varepsilon_p + m} \right) \qquad 4.3$$

Where, σ_r is the residual strength and ε_r is the corresponding strain.

Thus, the proposed model finally satisfies the last criterion and it is a complete model to simulate the nonlinear stress-strain relations of materials. From the proposed model we can see that a range of stress strain curves can be found depending on the initial gradient, which gives various a for the hardening part of the model. As a result various hardening stress strain curve can be simulated by varying the material parameter a. In the Figure 4.1 we can see a range of simulated normalized stress strain hardening curves by varying the material parameter a.

Similarly, a range of softening curves with various material parameter a by equating the equation of the curve at $\varepsilon = \varepsilon_r$ and $\sigma = \sigma_r$ can be found. In the Figure 4.2, we can see a range of simulated normalized stress strain softening curves by varying the material parameter m.

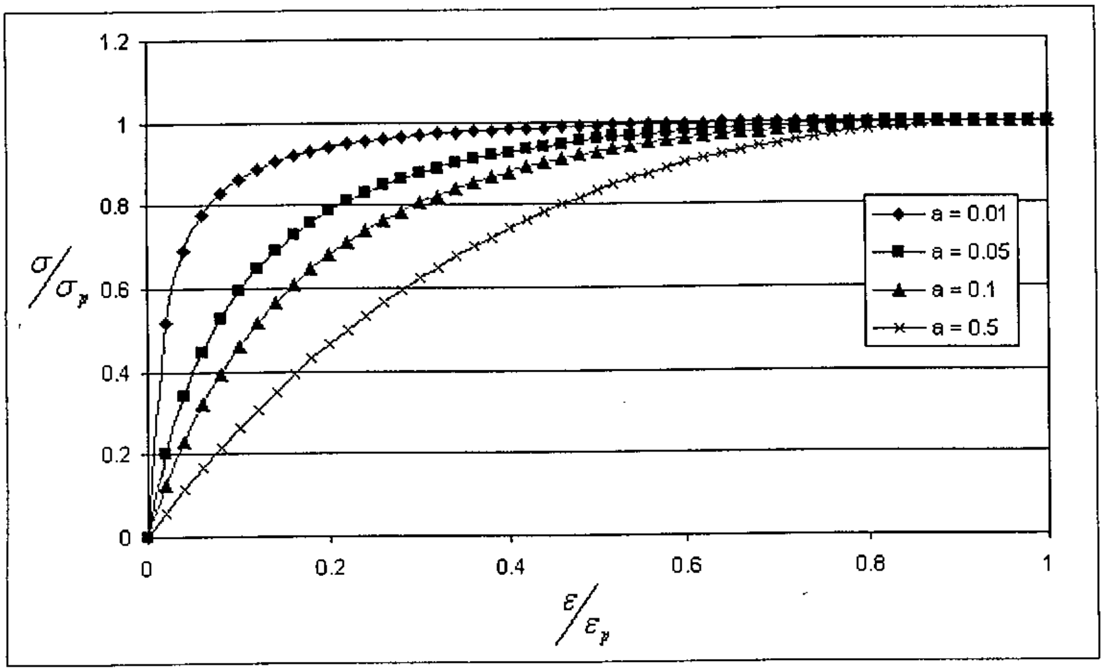

Figure 4.1: Normalized stress vs. normalized strain hardening curves for various a.

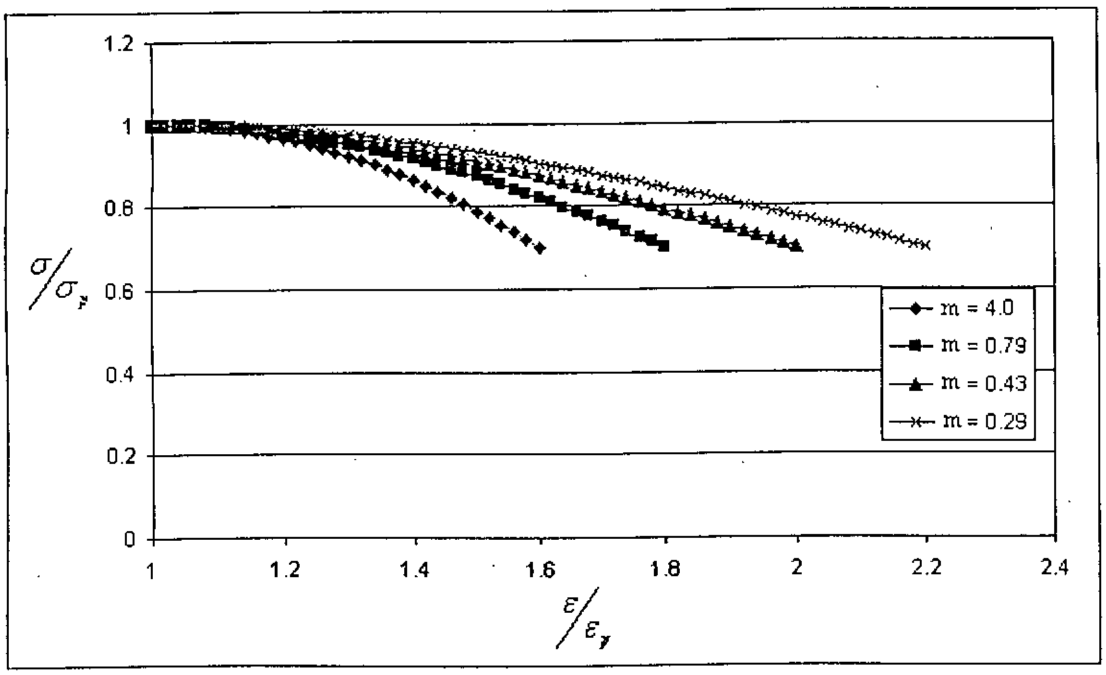

Figure 4.2: Normalized stress vs. normalized strain softening curves for various a.

Thus, we can see that the proposed model can well simulate a wide range of nonlinear stress-strain relations satisfying all the five criteria as mentioned above.

4.3 Evaluation of Kinematic Hardening Parameter *C*

By using the proposed nonlinear stress-strain relationship as the skeleton for the $\eta \sim \kappa$ relationship, the instantaneous slope of the curve following the proportional rule and drag rule gives the kinematic hardening parameter *C*. Thus, the loading and unloading skeleton $\eta \sim \kappa$ relation ship becomes,

$$\eta = f(\kappa) = \eta_{\max} \cdot \frac{\kappa_{\max} + a}{\kappa_{\max}^2} . \kappa . \left(\frac{\kappa_{\max} + a}{\kappa + a} - \frac{a}{\kappa_{\max} + a} \right) \text{ for loading} \qquad 4.4a$$

$$\eta = g(\kappa) = \eta_{\min} \cdot \frac{-\kappa_{\min} + a}{\kappa_{\min}^2} . -\kappa . \left(\frac{-\kappa_{\min} + a}{-\kappa + a} - \frac{a}{-\kappa_{\min} + a} \right) \text{ for unloading} \qquad 4.4b$$

Where, a is the material parameter which depends on the shape of the curve and can be evaluated from the initial kinematic hardening parameter C_0.

4.4 Pressure Independent Model

Since for the pressure independent materials the shear strength does not vary along the hydrostatic axis, a Von-Mises type cylindrical yield function is chosen as follows,

$$f = \sqrt{(S_{ij} - \alpha_{ij}) : (S_{ij} - \alpha_{ij})} = 0 \qquad 4.5$$

Where, the α_{ij} is the centre of the yield function and it evolves with the proposed kinematic hardening rule according to Equation 3.8 and S_{ij} is the deviatoric stress. In addition, due to the pressure independency an associative flow rule is used which means that the direction of the incremental plastic strain $d\varepsilon_{ij}^p$ is normal to the yield surface asfollows,

$$d\varepsilon_{ij}^p = \lambda \frac{df}{d\sigma_{ij}} \qquad 4.6$$

Where λ is the magnitude of the incremental plastic strain and $d\kappa = \lambda$.

4.5 Pressure Dependent Model

4.5.1 Yield Function

A Druker-Prager type conical pressure dependent yield surface is chosen as follows,

$$f = \sqrt{(S_{ij} - p\alpha_{ij}) : (S_{ij} - p\alpha_{ij})} = 0 \qquad 4.7$$

Where, the α_{ij} is the centre of the yield function, S_{ij} is the deviatoric stress and p is the hydrostatic pressure.

4.5.2 Stress-Dilatancy Relationship

An associative flow rule with a Druker-Prager type yield surface results an over predicted volumetric dilation. As a result, a non-associative flow rule becomes necessary. Again, for cyclic loading there exist two different rates of stress-dilatancy relations for loading and unloading directions at the same stress state. So, Tatsuoka et. al. [2003] proposed two different stress-dilatancy relations for loading and unloading. With some modification, the stress-dilatancy relationship becomes,

$$D = b.\frac{-\sin\phi_{mob}(1+1/K)+(1-1/K)}{\sin\phi_{mob}(1-1/K)+(1+1/K)} \text{ for loading} \qquad 4.8a$$

$$D = b.\frac{\sin\phi_{mob}(1+1/K)-(1-1/K)}{-\sin\phi_{mob}(1-1/K)+(1+1/K)} \text{ for unloading} \qquad 4.8b$$

Where, $D = \dfrac{d\varepsilon_v^p}{d\kappa}$.

$d\varepsilon_v^p$ is the incremental volumetric plastic strain, which is positive for compression and negative for dilation.

$d\kappa$ is the magnitude of the incremental plastic shear strain.

b and K are constants.

And the incremental plastic shear strain is given by,

$$de_{ij}^p = \lambda\frac{df}{dS_{ij}} \qquad 4.9$$

Where, $\lambda = d\kappa$.

4.5.3 Hardening Rule

The hardening rule as proposed (Equation 3.8) is modified for pressure dependent materials as follows,

$$d\alpha_{ij} = (1+d)Cde_{ij}^{p} \qquad 4.10$$

4.6 Summary

In this chapter, the formulation of the models for pressure independent and pressure dependent materials are given. To evaluate the instantaneous slope C, a nonlinear $\eta \sim \kappa$ relationship is required. Therefore, a simple nonlinear stress-strain model is proposed which can reasonably simulate a wide range of stress-strain relations for both hardening as well as softening parts. Then for the pressure independent materials, Von-Mises type cylindrical yield function is chosen with an associative flow rule. For pressure dependent materials a Druker-Prager type conical pressure dependent yield surface is chosen. Then the stress-dilatancy relationship proposed by Tatsuoka et. al. [2003] is incorporated to model the dilatancy behavior of pressure dependent materials.

CHAPTER 5
INTEGRATION ALGORITHM FOR THE CYCLIC PLASTICITY MODELS

5.1 Introduction

For relatively simple models, it is possible to obtain an analytical solution of differential equation that relates the stress rate to strain rate, but for more complicated models, numerical techniques must be employed. Although radial return methods (Wilkins [1964], Kreig and Kreig [1977]) and sub-incrementation techniques (Nayak and Zienkiewicz [1972]) have been proposed in early days, no firm algorithmic basis was available until the pioneering work of Ortiz and Popov [1985], Simo and Taylor [1986] and Ortiz and Simo [1986]. These semi-explicit algorithms are simple and efficient enough. In this chapter, the return mapping integration algorithm's application for both the pressure independent and pressure dependent materials are explained briefly.

5.2 Return Mapping Algorithm for Pressure Independent Model

The general form of the constitutive equations for pressure independent model are as follows:

$$f = \sqrt{(S_{ij} - \alpha_{ij}):(S_{ij} - \alpha_{ij})} = 0 \qquad 5.1a$$

$$d\varepsilon_{ij} = d\varepsilon_{ij}^{e} + d\varepsilon_{ij}^{p} \qquad 5.1b$$

$$d\varepsilon_{ij}^{p} = \lambda \frac{df}{d\sigma_{ij}} \qquad 5.1c$$

$$d\alpha_{ij} = (1+d)Cd\varepsilon_{ij}^{p} \qquad 5.1d$$

$$d\sigma_{ij} = D_{ijkl}^{e} d\varepsilon_{kl}^{e} \qquad 5.1e$$

$$f = f(\sigma_{ij}, \kappa) \qquad 5.1f$$

$$d\kappa = \lambda \qquad 5.1g$$

Let, $(\sigma_{ij}^{0}, \kappa^{0})$ state is within the elastic domain or upon the yield surface and the elastic stress update caused a jump outside the yield surface at $(\sigma_{ij}^{t}, \kappa^{t})$. Now, plastic corrector scheme is applied and finally the stress state is (σ^1_{ij},κ^1) where the yield function $f=0$. So we get,

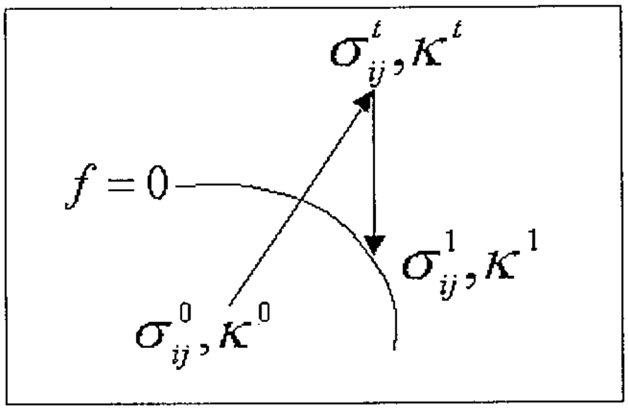

Figure 5.1: Geometric interpretation of return mapping algorithm

$$\sigma^1_{ij}-\sigma^0_{ij}=d\varepsilon_{kl}D^e_{ijkl} \qquad 5.2$$

$$\sigma^t_{ij}-\sigma^0_{ij}=d\varepsilon^e_{kl}D^e_{ijkl} \qquad 5.3$$

By subtracting Equation 5.2 from Equation 5.3 and using Equation 5.1,

$$\sigma^t_{ij}-\sigma^1_{ij}=(d\varepsilon_{kl}-d\varepsilon^e_{kl})D^e_{ijkl}$$

or, $$d\sigma_{ij}=d\varepsilon^p_{ij}D^e_{ijkl}$$

or, $$d\sigma_{ij}=D^e_{ijkl}\lambda\frac{\partial f}{\partial\sigma_{kl}} \qquad 5.4$$

By Tailor's series of expansion (1st order),

$$f(\sigma^t_{ij},\kappa^t)=f(\sigma^t_{ij},\kappa^0)-\frac{\partial f}{\partial\sigma_{ij}}d\sigma_{ij}-\frac{\partial f}{\partial\kappa}d\kappa \qquad 5.5$$

Here, because of the elastic move, κ^0 is used in the expansion process. Now, it is assumed that $f(\sigma^t_{ij},\kappa^t)=0$. By this step relaxation process and using Equation 5.4 we get,

$$f(\sigma^t_{ij},\kappa^0)-\lambda\frac{\partial f}{\partial\sigma_{ij}}D^e_{ijkl}\frac{\partial f}{\partial\sigma_{kl}}-\frac{\partial f}{\partial\kappa}d\kappa=0$$

$$\Rightarrow\lambda=\frac{f(\sigma^t_{ij},\kappa^0)}{\frac{\partial f}{\partial\kappa}+\frac{\partial f}{\partial\sigma_{ij}}D^e_{ijkl}\frac{\partial f}{\partial\sigma_{kl}}} \qquad 5.6$$

So, $$\sigma_{ij}^{1} = \sigma_{ij}^{\prime} - \lambda D_{ijkl}^{e} \frac{\partial f}{\partial \sigma_{kl}} \quad 5.7a$$

$$\alpha_{ij}^{1} = \int d\alpha_{ij} \text{ and } d\alpha_{ij} = (1+d)C\lambda \frac{\partial f}{\partial \sigma_{kl}} \quad 5.7b$$

$$\kappa^{1} = \int d\kappa \quad 5.7c$$

and C is constant for each load step.

Now, convergence check $f(\sigma_{ij}^{1}, \kappa^{1}) \le TOL|f|$

If the convergence is not satisfied, set $\sigma_{ij}^{1} \to \sigma_{ij}^{\prime}$, $\alpha_{ij}^{1} \to \alpha_{ij}^{\prime}$ and $\kappa^{1} \to \kappa^{\prime}$ the procedure should be followed again until the criteria is satisfied.

5.3 Return Mapping Algorithm for Pressure Dependent Model

The general form of the constitutive equations for pressure dependent model are as follows:

$$f = \sqrt{(S_{ij} - p\alpha_{ij}) : (S_{ij} - p\alpha_{ij})} = 0 \quad 5.8a$$

$$d\varepsilon_{ij} = d\varepsilon_{ij}^{e} + d\varepsilon_{ij}^{p} \quad 5.8b$$

$$\left(d\varepsilon_{ij}^{p}\right)_{s} = \lambda \frac{df}{dS_{ij}} \quad 5.8c$$

$$D = \frac{d\varepsilon_{v}^{p}}{d\kappa} \quad 5.8d$$

$$D = b.\frac{-\sin\phi_{mob}(1+1/K)+(1-1/K)}{\sin\phi_{mob}(1-1/K)+(1+1/K)} \text{ for loading} \quad 5.8e$$

$$D = b.\frac{\sin\phi_{mob}(1+1/K)-(1-1/K)}{-\sin\phi_{mob}(1-1/K)+(1+1/K)} \text{ for unloading} \quad 5.8f$$

$$d\alpha_{ij} = (1+d)C\left(d\varepsilon_{ij}^{p}\right)_{s} \quad 5.8g$$

$$d\sigma_{ij} = D_{ijkl}^{e} d\varepsilon_{kl}^{e} \quad 5.8h$$

$$f = f(S_{ij}, \kappa) \quad 5.8i$$

$$d\kappa = \lambda \quad 5.8j$$

Let, (S^0_{ij}, κ^0) state is within the elastic domain or upon the yield surface and the elastic stress update caused a jump outside the yield surface at (S'_{ij}, κ'). Now, plastic corrector scheme is applied and finally the stress state is (S^1_{ij}, κ^1) where the yield function $f = 0$. So we get,

$$S^1_{ij} - S^0_{ij} = 2Gde_{kl} \qquad 5.9$$

$$S'_{ij} - S^0_{ij} = 2Gde^e_{kl} \qquad 5.10$$

By subtracting Equation 5.9 from Equation 5.10 and using Equation 5.8,

$$S'_{ij} - S^1_{ij} = 2G(de_{kl} - de^e_{kl})$$

or, $$dS_{ij} = 2Gde^p_{ij}$$

or, $$dS_{ij} = 2G\lambda \frac{\partial f}{\partial S_{kl}} \qquad 5.11$$

And, $$p' - p^1 = d\varepsilon^p_v K^e$$

or, $$dp = d\kappa D K^e \qquad 5.12$$

Where K^e is the bulk modulus of elasticity.

By Tailor's series of expansion (1st order),

$$f(S'_{ij}, \kappa') = f(S'_{ij}, \kappa^0) - \frac{\partial f}{\partial S_{ij}} dS_{ij} - \frac{\partial f}{\partial \kappa} d\kappa - \frac{\partial f}{\partial p} dp \qquad 5.13$$

Here, because of the elastic move, κ^0 is used in the expansion process. Now, it is assumed that $f(S'_{ij}, \kappa') = 0$. By this step relaxation process and using Equation 5.11 and 5.12 we get,

$$f(S'_{ij}, \kappa^0) - \lambda \frac{\partial f}{\partial S_{ij}} 2G \frac{\partial f}{\partial S_{kl}} - \frac{\partial f}{\partial \kappa} d\kappa - \frac{\partial f}{\partial p} DK^e d\kappa = 0$$

$$\Rightarrow \lambda = \frac{f(S'_{ij}, \kappa^0)}{\frac{\partial f}{\partial \kappa} + \frac{\partial f}{\partial S_{ij}} 2G \frac{\partial f}{\partial S_{kl}} + \frac{\partial f}{\partial p} DK^e} \qquad 5.14$$

So,

$$S^1_{ij} = S'_{ij} - 2G\lambda \frac{\partial f}{\partial S_{kl}} \qquad 5.15a$$

$$p^1 = P' - \lambda D K^e \quad 5.15b$$

$$\alpha_{ij}^1 = \int d\alpha_{ij} \text{ and } d\alpha_{ij} = (1+d)C\lambda \frac{\partial f}{\partial S_{kl}} \quad 5.15c$$

$$\kappa^1 = \int d\kappa \quad 5.15d$$

and C is constant for each load step.

Now, convergence check $f(S_{ij}^1, \kappa^1) \le TOL|f|$

If the convergence is not satisfied, set $S_{ij}^1 \to S_{ij}'$, $p^1 \to p'$, $\alpha_{ij}^1 \to \alpha_{ij}'$ and $\kappa^1 \to \kappa'$, and the procedure should be followed again until the criteria is satisfied.

5.4 Summary

In this chapter, the implementation of the return mapping algorithm for both the pressure independent and pressure dependent materials are described. The return mapping algorithm is a very simple but efficient algorithm to integrate the incremental stress strain relationship. In each iteration, the algorithm checks the yield function. If the value of f is less than the tolerance limit $TOL|f|$, then it take the solution as a converged one. Otherwise, the final value of the previous iteration is used as initial values for the next iteration. In this iterative process, the stress and strains are integrated.

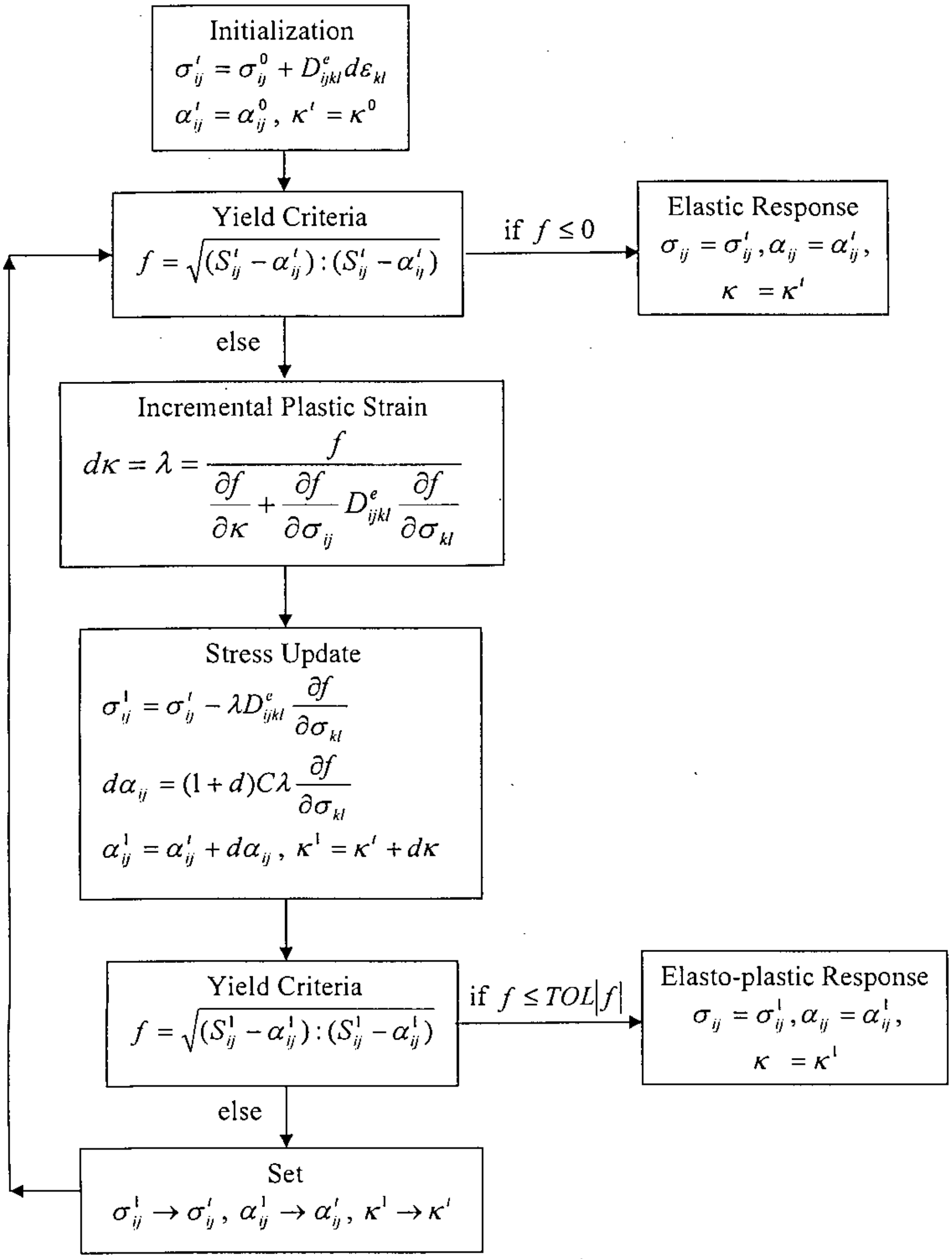

Figure 5.2: Flow Chart of Return Mapping Algorithm for Pressure Independent Materials

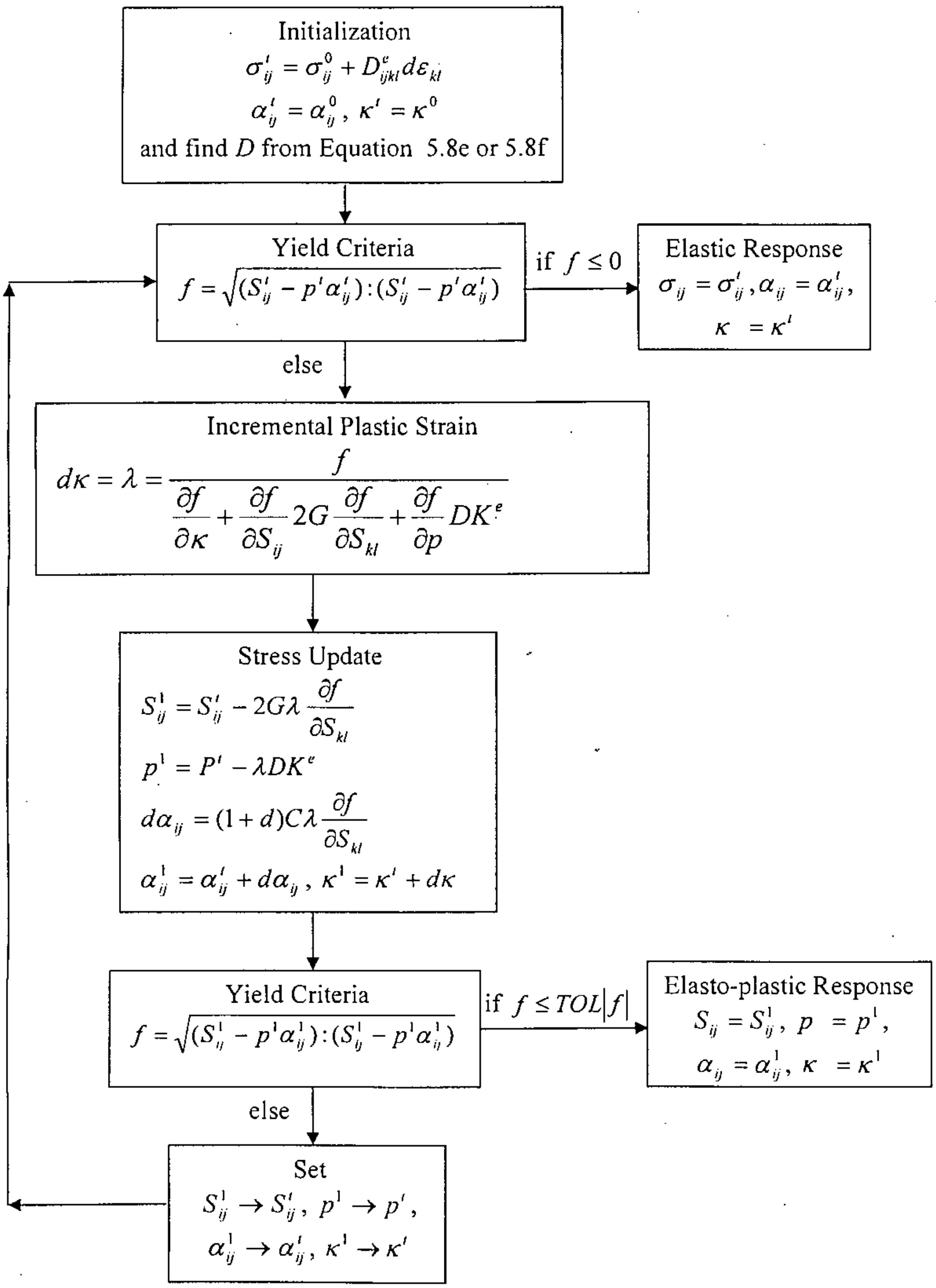

Figure 5.3: Flow Chart of Return Mapping Algorithm for Pressure Dependent Materials

CHAPTER 6
SOLUTION TECHNIQUE

6.1 Introduction

Dynamic Relaxation (DR) is based on the fact that a system undergoing damped vibration, excited by a momentum constrained force, ultimately comes to rest in the displaced position of static equilibrium of the system under the action of static force. As it attains a static solution through a dynamic process, it is sometime called 'pseudo-transient' or 'fictitious damping' process. Although this method of solution was initially developed as an alternative to linear solution techniques, its real force is its ability of solving the highly nonlinear geometric and material behavior. The explicit nature of the method makes it highly suitable for computations because all quantities may be treated as vectors resulting in an easily programmable method with low storage requirements. So explicit implementations of force level DR solvers have enjoyed success in treating problems with strong, sharp nonlinearities like non-associated flow in plasticity with large non-normality and very high friction angle.

6.2. General DR solution strategy

6.2.1. DR Equations

Governing equations of materially or geometrically nonlinear equation are given by

$$P - P^{init} = F$$

And $$P = \sum_{N} \int_{ve} B^{T} \sigma dv \qquad 6.1$$

Where,

P is the vector of internal forces

P^{init} is the vector of nodal forces due to initial stresses.

F is the vector of external forces.

B is the displacement-strain transformation matrix.

N is the number of elements in the FEM discretization.

$\sum$ is the vector of stresses in each element.

ve is the volume of the each element.

The solution to the above governing equations is presented by obtaining the steady state response of a dynamic equation of motion:

$$m\ddot{u} + c\dot{u} + P - P^{init} = F \qquad 6.2$$

Where,

m is the mass matrix.

c is the damping matrix.

$\ddot{u}$ is the acceleration vector, and,

$\dot{u}$ is the velocity vector.

Applying the central difference technique to Equation 6.2, we get;

$$\dot{u} = \frac{u^{t+\Delta t} - u^{t-\Delta t}}{2\Delta t} \qquad 6.3$$

$$\ddot{u} = \frac{u^{t+\Delta t} - 2u^{t} + u^{t-\Delta t}}{(\Delta t)^2} \qquad 6.4$$

where, Δt is the time increment.

Using a diagonal mass matrix m, the damping matrix is determined as:

$$c = \alpha m \qquad 6.5$$

where, α is the damping ratio.

Substituting Equation 6.3, 6.4, and 6.5 into Equation 6.2, we get,

$$u^{t+\Delta t} = \frac{1}{(1+0.5\alpha\Delta t)}\left[\frac{\Delta t^2}{m}\left(F - P + P^{init}\right) + 2u^{t} - (1-0.5\alpha\Delta t)u^{t-\Delta t}\right] \qquad 6.6$$

The above equation is a time marching equation, which has to be solved explicitly. Hence, a limitation of the critical time step is imposed on this equation, which will be discussed in the subsequent sections.

6.2.2 Damping parameter determination

In the dynamic relaxation method, the determination of the damping value is the most critical one. If an arbitrary damping factor is given, a large amount of computer time is necessary to get the damped static value. So many researchers have suggested various methods to determine the nearly critical damping factor

The following method, estimated by Rayleigh's quotient, is proposed by Bunce [1972] and is frequently used in computation of critical damping parameter:

$$c = 2\sqrt{\frac{x^T \mathrm{K} x}{x^T m x}} \qquad 6.7$$

where,

x is the eigenvectors (incremental displacement is also acceptable for approximate damping factor)

K is the diagonal stiffness matrix.

m is the mass matrix.

The Rayleigh's norm is proposed mainly for linear analysis. For nonlinear problem, the same expression as in Equation 6.7 can be used by selecting the nodal displacement vector u and the local tangent stiffness matrix K. The tangent stiffness matrix K is approximated by the diagonal form:

$$\mathrm{K} = \frac{{}^{t}P - {}^{t-\Delta t}P}{\Delta t \cdot {}^{t}\dot{u}} \qquad 6.8$$

where, ${}^{t}P$ and ${}^{t-\Delta t}P$ are components of the internal force vector at time t and $t-\Delta t$, respectively and ${}^{t}\dot{u}$ is a component of the velocity vector at time t.

6.2.3 Stabilization and optimization

The dynamic relaxation scheme is an explicit formulation and all the explicit time-wise integration procedure which uses the central difference formula is only conditionally stable. In many cases this restricts the choice of the time interval to very small values if numerical instability is to be avoided. It has a definite limit of time step beyond which the solution method becomes unstable. This is governed by the well-known Courant-Friedrichs-Levy condition. Actually it says that Δt can not be larger than the time taken by the two adjacent nodes of the mesh to transfer the information of deformation. This instability arises mainly from the mismatch of integration speed and deformation wave speed. Mathematically this condition can be expressed as:

$$\Delta t \le \beta \frac{l}{V_c} \qquad 6.9$$

Where, β is a factor to control the stability and speed of computation $(\beta \le 1.0)$. l is the minimum distance between the adjacent nodal points for an element. For constant strain elements, the value of β can be near 1.0, but for higher order elements it reduces very fast. V_c is the constrained compression wave velocity of the medium, since the pseudo densities are calculated separately in each of the x and y directions. From Equation 6.9 we get the following expression,

$$\Delta t = l\beta \sqrt{\frac{\rho(1+\nu)(1-2\nu)}{E(1-\nu)}} \qquad 6.10$$

Following the above equation, the stability of the integration of the equation of motion can be assured but the critical time for stability may be too short, thus too conservative. So various forms of fictitious mass are introduced in order to increase the convergence rate towards the static solution.

The most effective method for determining the elements of m is to choose m_{ii} in such a way that the transit time for deformation wave for the degree of freedom 'i' to the adjacent and similar degrees of freedom remains constant. Usually this constant is linked to the time step, $\Delta t = 1$. So, m_{ii} is determined in such a way that Δt is always equal to 1 according to the stiffness of the medium through which deformation wave is proceeding (Cassel and Hobbs [1976]).

Based on Equation 6.10 a scaling method is introduced. An artificial mass density ρ is calculated from Equation 6.10 on the element by element basis so as to give the same transit time across each element for any element size. In this way, deformation information (unbalance forces) travels uniformly over the whole mesh irrespective of different size elements. In this way, the computational speed can be maximized by minimizing the ratio of maximum to minimum eigenvalues of the system. So, from Equation 6.10, taking $\Delta t = 1$, we can have the fictitious density for the pseudo-mass matrix:

$$\rho = \frac{E(1-\nu)}{\beta^2 l^2 (1+\nu)(1-2\nu)} \tag{6.11}$$

Where, E is the Young's modulus of elasticity, ν is the Poisson's ratio. l is the minimum between the adjacent nodes of an element in the finite element mesh. ρ is the fictitious density varying from element to element in the FEM mesh. It is already described that β is a factor $(0 < \beta < 1)$ controls the speed of convergence. $\beta = 1$ means that the integration speed will have maximum speed and $\beta \approx 0.0$ means that it will have the lowest speed. In all of the numerical tests described in later chapter, the only adjustable DR parameter was β, which was set equal to 0.6 to achieve the stability of the explicit DR computation. All the other parameters were adapted and adjusted automatically through the equilibrium iterations.

6.3. Tracing equilibrium path

In this section, the DR method is evaluated from the viewpoint of its ability in tracing the whole equilibrium curve in the load-displacement space exhibiting post-peak softening. In the case of material nonlinearity usually there is a snap-through. The direct displacement control strategy that was applied to trace the whole equilibrium path is described in the following section.

6.3.1. Displacement control strategy

In the displacement control solution, some of the displacement components are fixed during one load step while the others are solved. Equations for fixed displacement components are as follows:

$$u^{t+\Delta t} = \delta_1 \left(m^t R^t + 2u^t - \delta_2 u^{t-\Delta t} \right) \tag{6.12(a)}$$

$$R^{t-\Delta t} = 0, \delta_1 = \delta_2 = 1.0, u^t = u^{t-\Delta t} \tag{6.12(b)}$$

Where,

$$\delta_1 = \frac{1}{(1 + 0.5\alpha\Delta t)},$$

$$\delta_2 = 1 - 0.5\alpha\Delta t \ ,$$

$$m' = \frac{\Delta t^2}{m} \text{, and,}$$

$$R' = \left(F - P + P^{init}\right)$$

6.4. Stress updating

In the way of the solution of the non-linear incremental equilibrium equations, the elasto-plastic incremental stress-strain relations are integrated. This integration is based on either incremental or iterative strains. Here incremental stress update is used.

Incremental stress update is on the incremental strain update. Due to solution procedure (DR), incremental strain has to be calculated from the last equilibrium position. Obviously, in incremental stress update more CPU is used due to the large incremental strain (stress). However, with a good elasto-plastic incremental stress-strain integrating tool, it produces more accurate results.

6.5 Summary

Solution techniques are discussed in this chapter. Especially, the method of Dynamic Relaxation (DR) technique is explained in details. As the results of any nonlinear FEM depends on the efficiency and accuracy of the solution method, so the stabilization, optimization and damping parameter determinations of DR solution technique are discussed here. Finally, displacement control strategy is discussed which is faster than any other schemes.

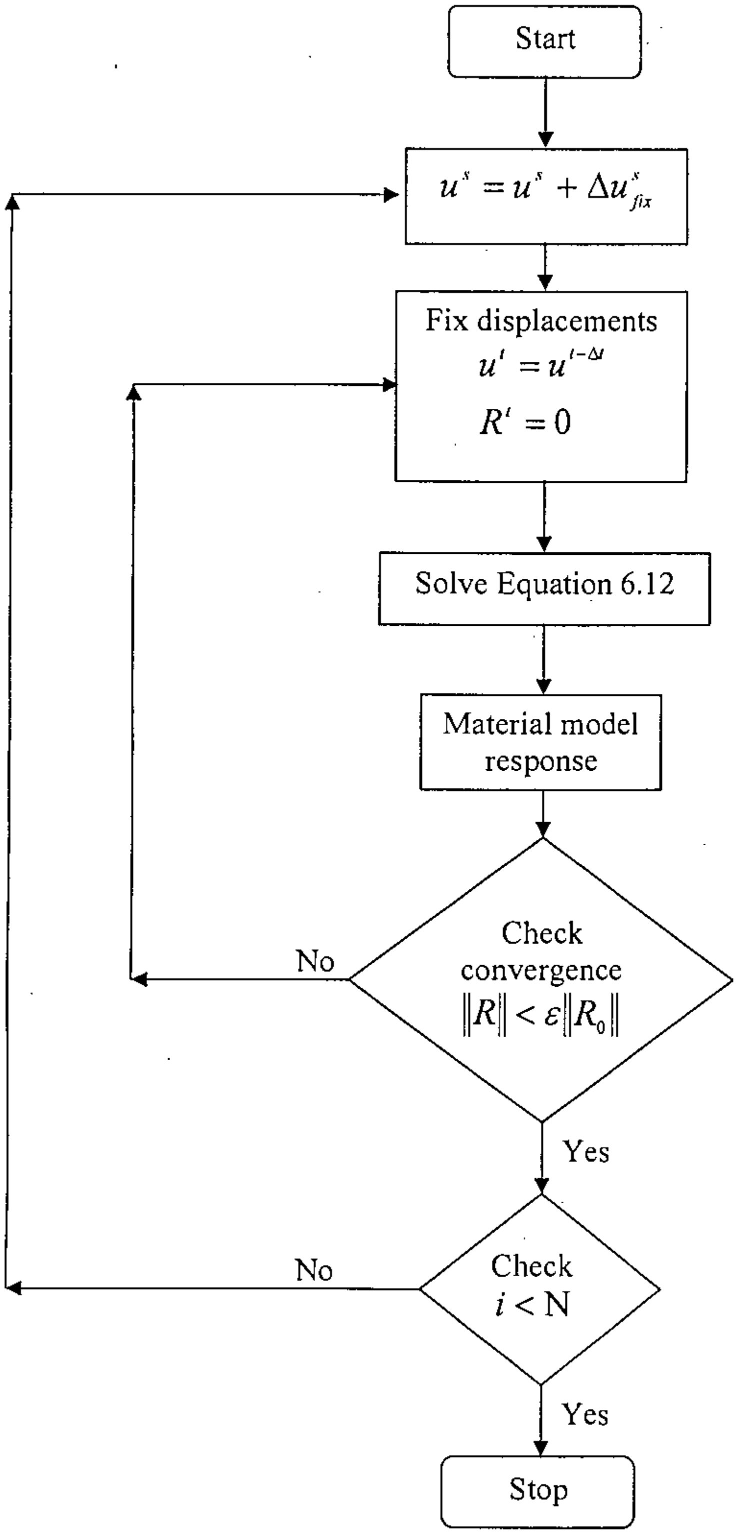

Figure 6.1: Flow Chart for Displacement Control Solution technique

CHAPTER 7

SIMULATION OF CYCLIC PLANE STRAIN RESPONSE

7.1 Introduction

The proposed constitutive models can well simulate the cyclic stress stain behavior of both the pressure independent materials like concrete and pressure dependent materials like sand. In this chapter, parametric studies are made both for the pressure independent and pressure dependent materias. Moreover, Masuda et. al. [1999] performed a series of plane strain cyclic loading tests on Toyoura sand and Tatsuoka et. al. [2003] proposed a nonlinear stress-strain relationship to simulate these test results. Here, these test results are simulated with the proposed model for pressure independent materials. For numerical simulation single element is used and for the nonlinear iterative solution of the governing equations Dynamic Relaxation algorithm is used. Then, the incremental stress-strain relationship is integrated using Return Mapping algorithm. The description of the Return Mapping algorithm and Dynamic Relaxation algorithm are given in chapter 6 and chapter 7 respectively.

7.2 Choice of Element

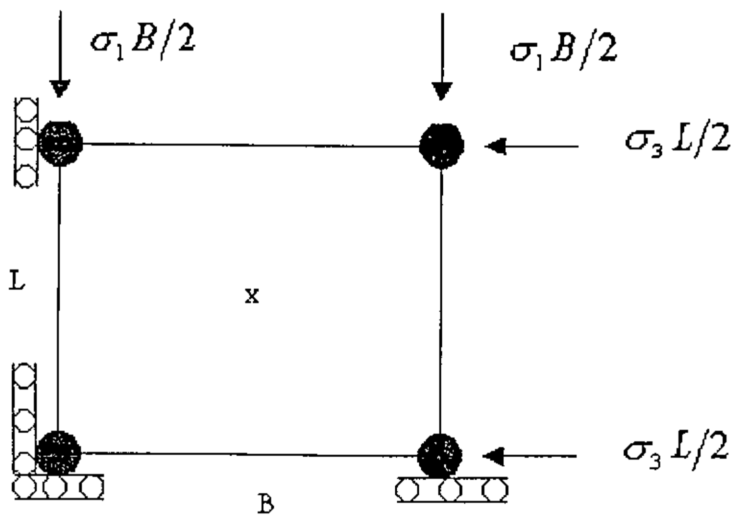

Figure 7.1: Quadrilateral Element

For comprehensive analysis of the numerical scheme, a relatively simple problem is selected. In the context of FEM, it is a four-noded quadrilateral (Figure

7.1) plane strain element is chosen here. This element has four degree of freedoms. The confining pressure σ_3 is kept constant to simulate the plane strain behavior. Moreover, only single point Gauss Quadrature integration is chosen to integrate the incremental stress-strain relation.

7.3 Parameter Determination

The model parameters $\eta_{max/min}$ and the material parameters $\kappa_{max/min}$ are required to calculate the instantaneous slope C of the kinematic hardening rule. The material parameters κ_{max} and κ_{min} represents the maximum cumulative plastic shear strain and have a direct relevance with the shear strain γ_{max} and γ_{min}. So, κ_{max} and κ_{min} can be directly determined from the test results. The model parameters η_{max} and η_{min} are the internal parameters for the background algorithm. For pressure independent model, η_{max} and η_{min} has direct relevance with the stress ratio R_{max} and R_{min}. The relationship $R \sim \kappa$ and $\eta \sim \kappa$ are shown in Figures 7.2 and 7.3. So, η_{max} and η_{min} can be determined by developing a regression equation relating them with R_{max} and R_{min} respectively.

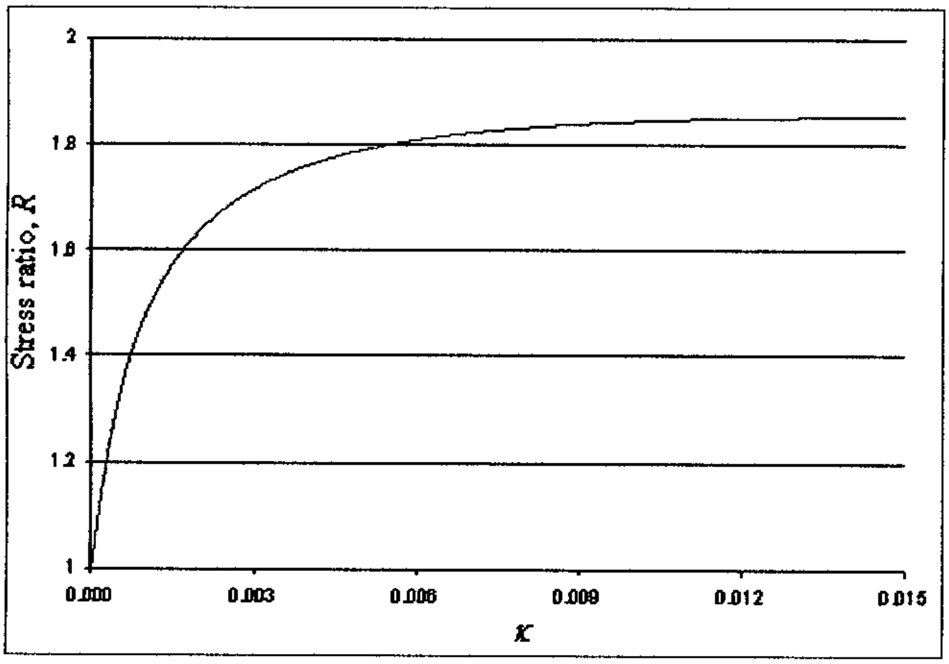

Figure 7.2: $R \sim \kappa$ relationship

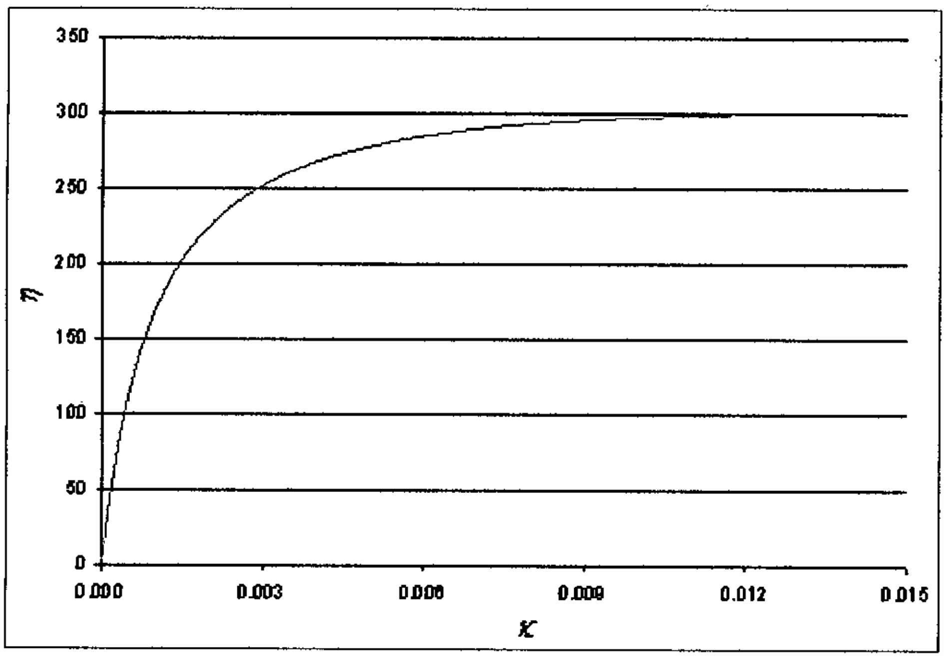

Figure 7.3: $\eta \sim \kappa$ relationship

For pressure dependent model, η_{max} and η_{min} has direct relevance with the stress ratio $Sin\phi_{max}$ and $Sin\phi_{min}$. The relationship $Sin\phi \sim \kappa$ and $\eta \sim \kappa$ are shown in Figures 7.4 and 7.5. So, η_{max} and η_{min} can be determined by developing a regression equation relating them with $Sin\phi_{max}$ and $Sin\phi_{min}$ respectively.

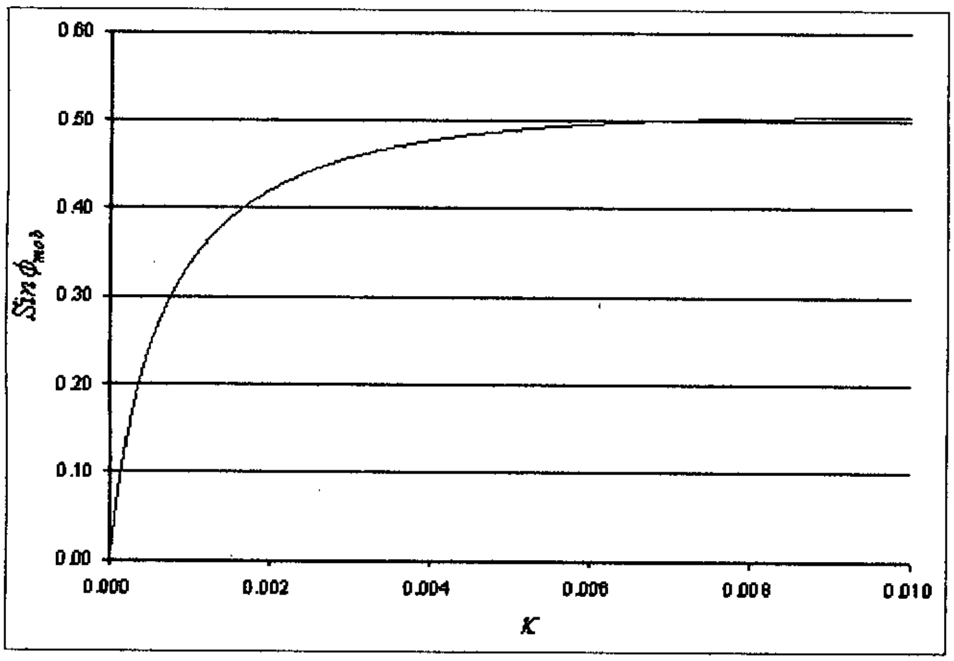

Figure 7.4: $Sin\phi \sim \kappa$ relationship

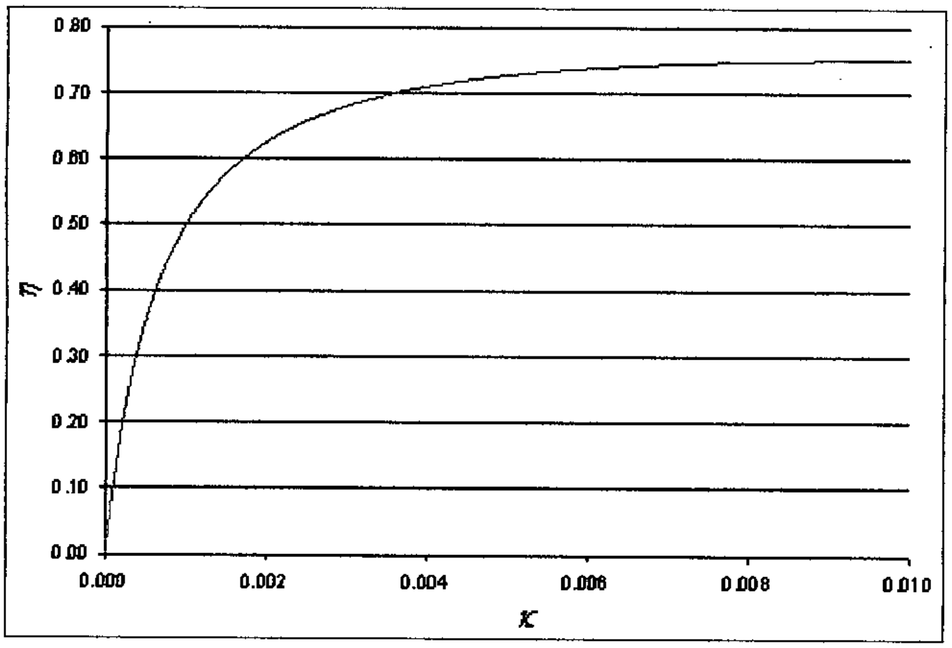

Figure 7.5: $\eta \sim \kappa$ relationship

7.4 Parametric Study of the Pressure Independent Model

Stress levels of Materials like concrete are not depend on the mean pressure level. Therefore, a pressure independent model like the proposed one is adequate to simulate the cyclic stress strain behavior. For the parametric study of the proposed pressure independent model a range of the parameters are chosen. The elastic parameters are kept constant and a symmetric loading and the unloading curves are selected for this parametric study ignoring the drag rule. The $R \sim \gamma$ relationship is found as closed loop in this simulation.

Table 7.1: Material Parameters

Shear Modulus of Elasticity, G	642,890 psi
Bulk Modulus of Elasticity, K^e	538,990 psi
Confining Pressure, σ_3	500 psi
$\kappa_{max/min}$	0.015

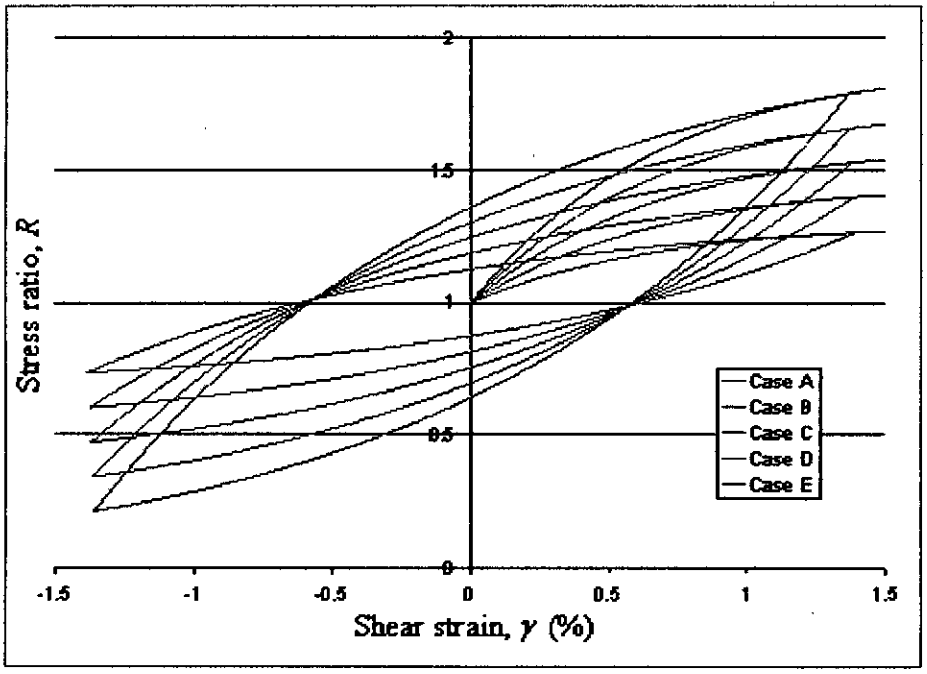

Figure 7.6: Variation of $R \sim \gamma$ relationship with varying $\eta_{max/min}$

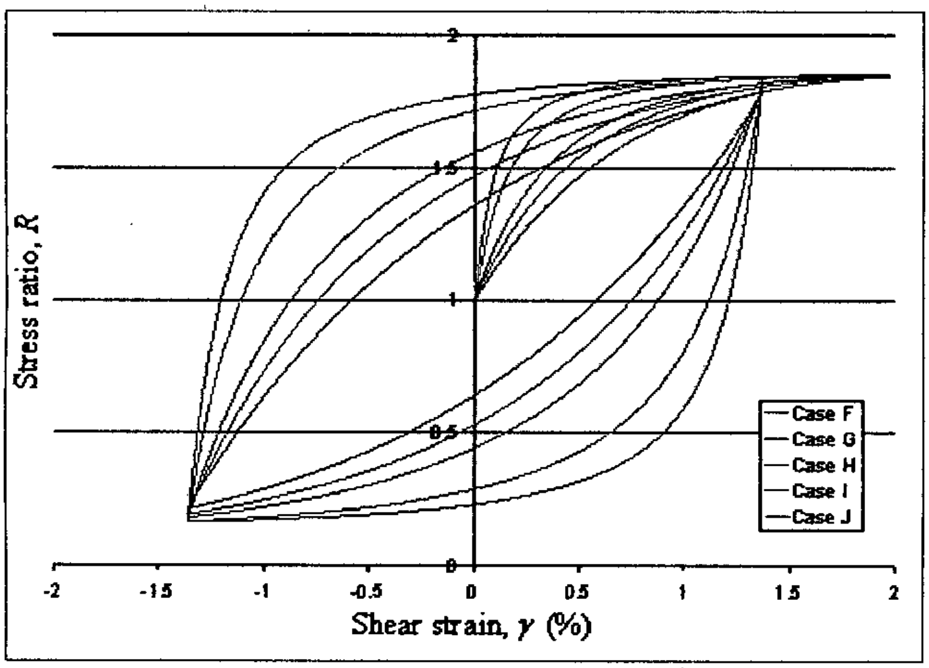

Figure 7.7: Variation of $R \sim \gamma$ relationship with varying a

Table 7.2: Model parameters

	$\eta_{max/min}$	a		$\eta_{max/min}$	a
Case A	300		Case F		0.01
Case B	250		Case G		0.005
Case C	200	0.01	Case H	300	0.003
Case D	150		Case I		0.001
Case E	100		Case J		0.0005

7.5 Parametric Study of the Pressure Dependent Model

For materials like sand, the stress-strain relationship is dependent upon the mean pressure level of the material. As a result, proposed pressure dependent model is appropriate for this kind of materials. In case of the parametric study for the pressure dependent material, the effect of various stress-dilatancy parameter upon the stress-strain relationship as well as stress-dilatancy relationship are simulated. Here unsymmetric loading and unloading skeleton curves are chosen to simulate the stress-strain response. The $Sin\phi_{mob} \sim \gamma$ relationship is found as nearly closed loop in this simulation and the stress-dilatancy simulation results showed reasonable simulation.

Table 7.3: Material and model parameters

Confining Pressure, σ_3	540 psi
$\kappa_{max/min}$	0.01
η_{max}	0.75
η_{min}	0.99
a	0.0007
b	1.0/3.0

Table 7.4: Variable material and model parameters

	Shear Modulus of Elasticity, G	Bulk Modulus of Elasticity, K^e	K for loading	K for unloading
Case K	642,890 psi	538,990 psi	3.5	3.5
Case L			3.5	1.8
Case M			1.8	3.5
Case N			1.8	1.8
Case O			1.0	1.0
Case P	1068380 psi	1262630 psi	3.5	3.5
Case Q	642,890 psi	538,990 psi		
Case R	341800 psi	404040 psi		
Case S	530,770 psi	1,150,000 psi		

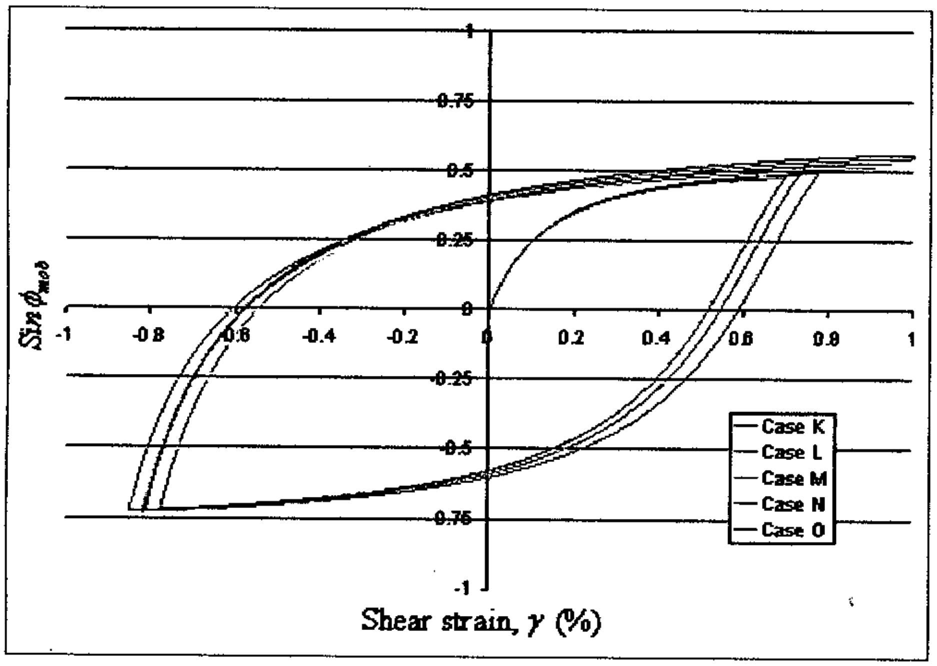

Figure 7.8: Variation of $Sin\phi_{mob} \sim \gamma$ relationship with varying K

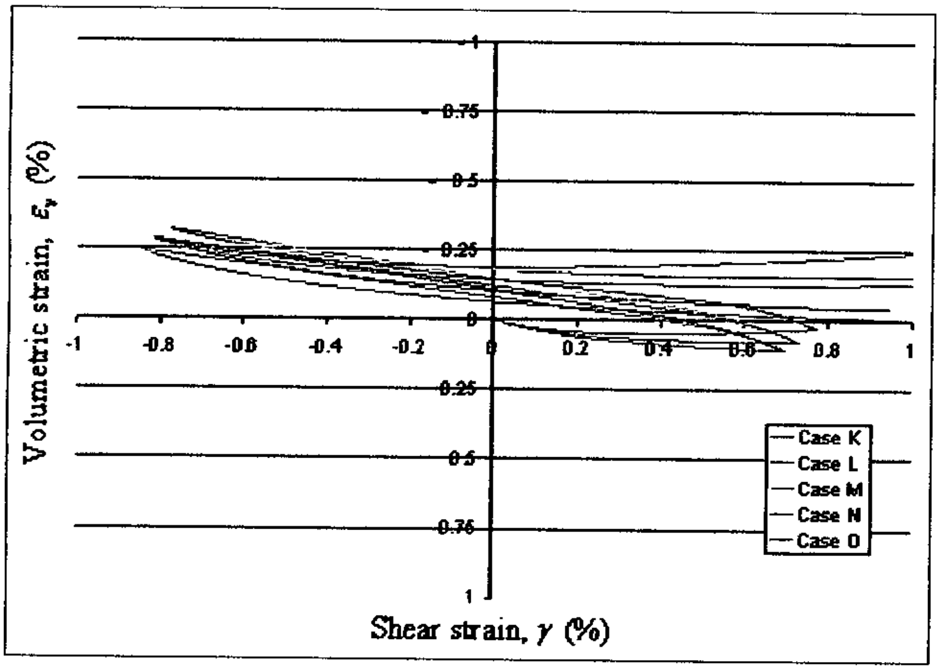

Figure 7.9: Variation of $\varepsilon_v \sim \gamma$ relationship with varying K

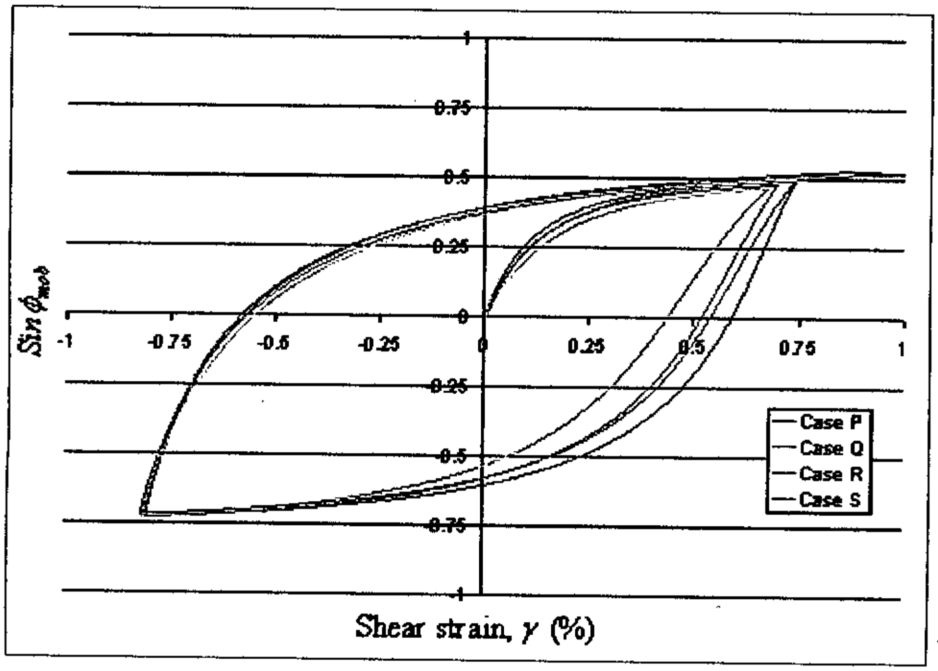

Figure 7.10: Variation of $Sin\phi_{mob} \sim \gamma$ relationship with varying G and K^e

7.6 Simulation of Cyclic Plane Strain Response

The stress-strain relationship of the Toyoura sand is simulated with the proposed model and compared with the results of Masuda et. al. [1999]. The plane strain compression and extension skeleton curves from the experiment results were not symmetrical and the loops of the $Sin\phi_{mob} \sim \gamma$ relation ship were not closed. So, due to the pressure dependency and to simulate the test results a drag rule is applied. Also, to simulate the stress-dilatancy relationship a stress-dilatancy rule is applied (Tatsuoka et. al. [2003]). The material and the model parameters given in the Table 7.3 and 7.4 of the Case K and the drag parameter d is evaluated using the following algorithm,

For loading and unloading skeleton curve:

The hardening rule: $d\alpha_{ij} = Cde^{p}_{ij}$

Otherwise:

The hardening rule: $d\alpha_{ij} = (1+d)Cde^{p}_{ij}$ *with*

for loading curve: d = 0

for unloading curve: d = 0.011

The simulated $Sin\phi_{mob} \sim \gamma$ and $R \sim \gamma$ relationships are given in the Figures. 7.7 and 7.8. Finally, the volumetric strain vs. shear strain relationship is given in the Figure. 7.9.

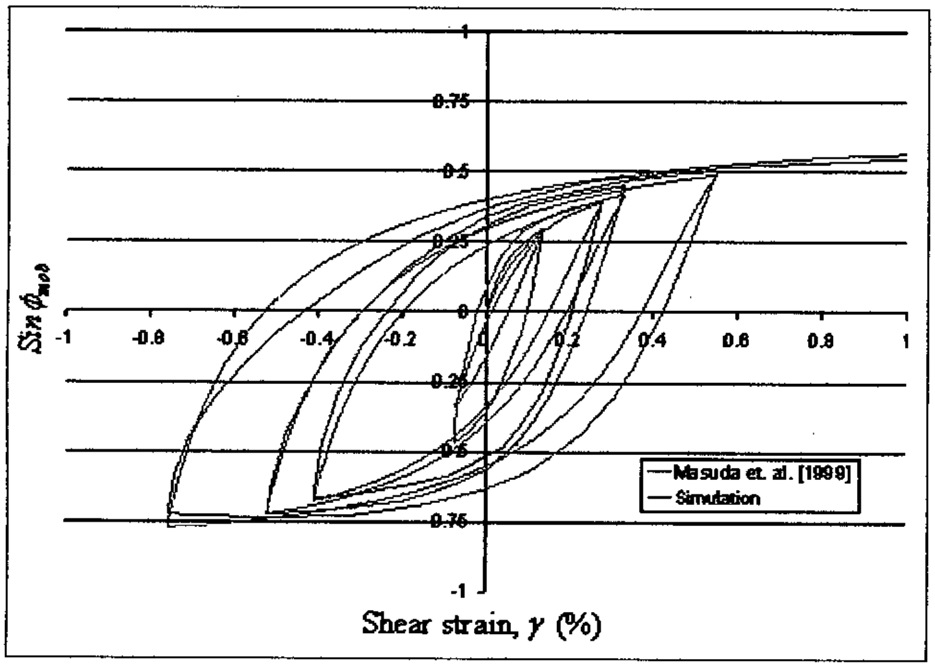

Figure 7.11 Comparison of $Sin\phi_{mob} \sim \gamma$ relationship between the test result and the simulation

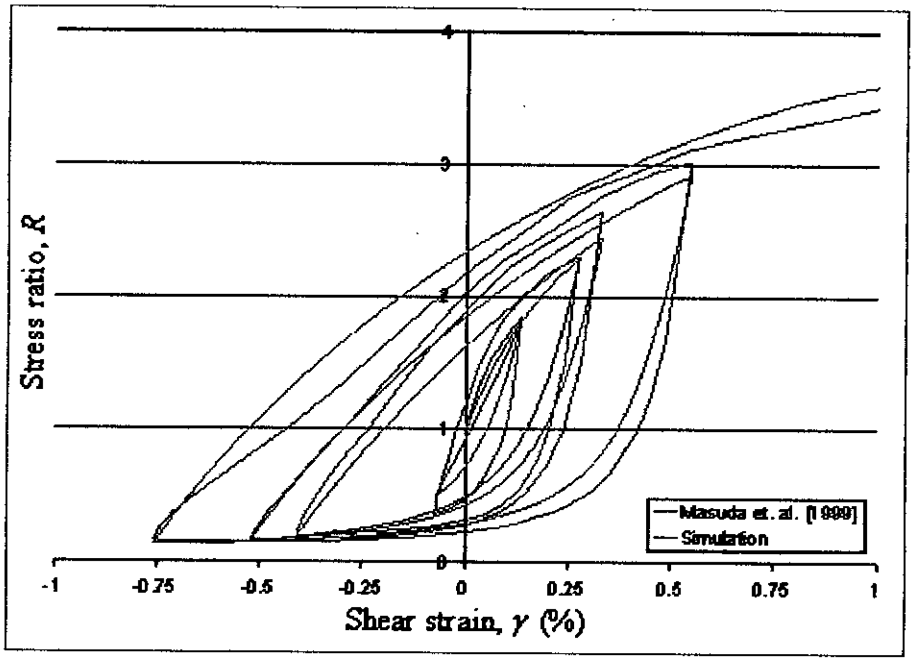

Figure 7.12 Comparison of $R \sim \gamma$ relationship between the test result and the simulation

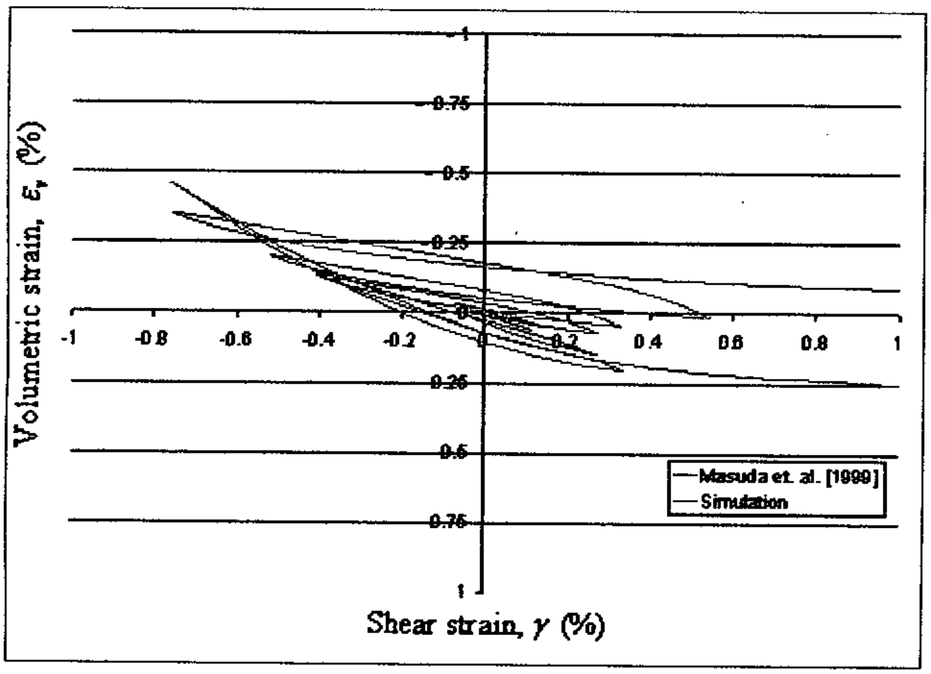

Figure 7.13 Comparison of $\varepsilon_v \sim \gamma$ relationship between the test result and the simulation

7.7 Summary

In this chapter, a finite element plane strain simulation is made with the proposed model. In this regard, parametric study is made for both the pressure dependent and pressure independent models. Moreover, a simulation is made for the Toyoura sand which is a pressure dependent material. Masuda et. al. [1999] performed a series of plane strain cyclic loading tests on Toyoura sand and Tatsuoka et. al. [2003] proposed a nonlinear stress-strain relationship to simulate these test results. The simulation results shows a good correlation with the stress-strain relationship. Also, the stress-dilatancy relationship is simulated using the model.

CHAPTER 8
CONCLUSIONS

8.1 Summary

Mathematical modeling of the constitutive relationship of materials is an essential part of the numerical modeling of engineering structures. In the present research, a robust cyclic constitutive model for pressure dependent and pressure independent elasto-plastic materials is developed. Firstly, a general framework for the cyclic modeling has been proposed. In this framework, a nonlinear kinematic hardening is derived from the concept of the instantaneous slope of the stress-strain relationship. For this purpose a proportional rule and a drag rule is formulated. By using the proportional rule, the modified Masing's rule is fulfilled as the cyclic evaluation some times resembles this feature. Using the drag rule, the overshooting or the undershooting of the stress-strain relationship can be modeled. Then a nonlinear stress-strain relationship is indispensable to develop a constitutive model which is simple but fulfills all the necessary requirements. Using this equation the instantaneous slope is calculated. By using this instantaneous slope for kinematic hardening rule, models for both the pressure independent and dependent materials have been developed. The Von-Mises and Druker-Prager yield functions were used for pressure independent and pressure dependent materials respectively. Then an associative flow rule is adopted for the pressure independent material where as a stress-dilatancy rule proposed by Tatsuoka et. al. [2003] is used with some modification. For the integration of the of the incremental stress-strain relationships Return Mapping algorithm is used (Ortiz and Popov [1985], Simo and Taylor [1986] and Ortiz and Simo [1986]) and for the nonlinear solution of the finite element analysis Dynamic Relaxation technique is used. Finally, to verify the model, a single four node quadrilateral element is chosen with single gauss point integration and a plane strain simulation is made. Masuda et. al. [1999] performed a series of plane strain cyclic loading tests on Toyoura sand. In this research, an attempt is made to simulate the cyclic plane strain behavior of Toyoura sand and the result was found quit reasonable. Thus the proposed model can be applicable for any type of structural as well as soil-structure interaction problems.

8.2 Conclusions

The proposed model is based on a generalized framework of kinematic hardening rule which has been developed by replacing the constant of Prager's kinematic hardening rule with an instantaneous slope found from a nonlinear skeleton curve. This concept gives rise to a robust framework in the field of the cyclic plasticity modeling. The significance of the proposed model is stated as follows

- The proposed model has the ability to simulate fully nonlinear cyclic stress-strain behavior of engineering materials.
- It has the ability to correctly model the Masing's Rule and its extension and can simulate closed loop cyclic stress-strain behavior.
- The proposed model can simulate the cyclic stress-strain behavior of both the pressure independent materials like concrete and pressure dependent materials like sand with good precision.
- Finally, using a stress-dilatancy relationship, the volume-changing behavior of the pressure dependent materials can be well simulated.

8.3 Scope of Future Research

The present research has the potentials for opening a new avenue for researchers involved in constitutive modeling of materials. Future research can be made in the following fields:

- Using the present framework, a new type of curved yield faction can be incorporated to overcome the limitations of the Druker-Prager yield function.
- More accurate stress-dilatancy relationship can be developed to simulate the volumetric strain of pressure dependent materials under cyclic loading.
- Instead of the semi-explicit integration algorithm like Return Mapping algorithm, an implicit integration algorithm can be incorporated to integrate the incremental stress-strain relationship for large load step and for better accuracy.
- Finally, the model can be incorporated into any finite element code to simulate structural as well as soil-structure interaction problems under cyclic loading.

REFERENCES

Ahmad, S. I. (2002), "Development of 3D Generalized Lattice Equivalent Continnum Model for Analysis of Reinforced Concrete Structures", D. Eng. Dissertation, Nagoya University, Japan.

Al-Karni, A. and Alshenawy, A. (2006), "Modeling of stress-strain curves of drained triaxial test on sand", American Journal of Applied Sciences 3 (11), 2108-2113,2006.

Armstrong, P.J. and Frederick, C.O. (1966), "A Mathematical Representation of the Multiaxial Bauscinger Effect", CEGB Report No. RD/B/N 731

Bari. S. (2001), "Constitutive modeling for cyclic plasticity and ratcheting", Ph. D. Thesis, Dept. of Civil Engineering, North Carolina State University.

Bunce, J. W. (1972), "A Note on the Estimation of Critical Damping in Dynamic Relaxation", International Journal of Numerical Methods in Engineering, 4, 301-304

Cassel A. C. et al. (1968), "Cylindrical Shell Analysis by Dynamic Relaxation", Proceedings of Institute of Civil Engineers, 39, 75-84

Cassel, A. C. and Hobbs, R. E., (1976), "Numerical Stability of Dynamic Relaxation Analysis of Non-linear Structure", International Journal of Numerical Methods in Engineering, 10, 1407-1410

Chaboche, J.L. (1986), "Time Independent Constitutive Theories for Cyclic Plasticity," Int. J. Plasticity, 2, 149.

Chaboche, J.L., 1991. On some modifications of kinematic hardening to improve the description of ratcheting effects. Int. J. Plasticity. 7, 661-678.

ChabocheL J.L., Dang Van, K., and Codier, G. (1976), "Modelization of the Strain Memory Effects on the Cyclic Hardening of 316 Stainless Steel," Trans. 5th Int. Conf. on Structural Mechanics in Reactor Technology, Vol. L, August 1979, Berlin, Paper No. L 11/3, North-Holland, Amsterdam.

Chen, W. F (1982), "Plasticity in Reinforced Concrete", McGraw-Hill, New York.

Chen, X., Jiao, R., 2004. Modified kinematic hardening rule for multiaxial ratcheting prediction, International Journal of Plasticity. 20, 871–898.

Crisfield, M. A. (1981), "A Fast Incremental/Iterative Procedure that Handles Snap-through", Computers and Structures, 13, 55-62.

Dafalias, Y. F., and Popov, E. P. (1975). ''A model of nonlinearly hardening materials for complex loadings.'' Acta Mech., 21, 173–192.

Dafalias, Y. F., and Popov, E. P. (1976), "Plastic Interal Variables formalism of Cyclic Plasticity", J. Appl. Mech., 98(4), 645-650

Dafalias, Y.F., Manzari, M.T., (2004)," Simple Plasticity Sand Model accounting for Fabric Change Effects", Journal of Engineering Mechanics, Vol. 130, No. 6

Day, A. S. (1965), "An Introduction to Dynamic Relaxation", Engineer, 219, 218-221.

Drucker, D. C. (1951), "A More Fundamental Approach to Plastic Stress-Strain Relations", Proc. 1st Natl. Congr. Appl. Mech. ASME, Chicago, 1951, 487-491.

Druker, D. C. and Prager, W. (1952), "Soil mechanics and plastic analysis or limit design", Q. Appl. Math. 10(2), 157-175.

Felippa, C. A. (1986), "Dynamic Relaxation and Quasi-Newton Methods", Numerical Methos for Non-Linear Problems, Swansea, 27-38

Griffith, D.V. and Prevost, J.H. (1990), "Stress strain curve generation from simple triaxial parameters", International Journal for Numerical and Analytical Methods in Geomechanics, Vol. 14, 587-594, 1990.

Hashiguchi, K. and Chen, Z. P. (1998). "Elastoplastic constitutive equation for soils with the rotational hardening", Int. J. Numer. Anayt. Meth. Geomech., Vol. 22, 197-222.

Hashiguchi, K. and Tsutsumi, S, (2001), "Elastoplastic Constitutive Equation with Tangential Stress Rate Effect", International Journal of Plasticity 17 (2001) 117-145

Hashiguchi, K., 1980. Constitutive equations of elastoplastic materials with elastic-plastic transition. J. Appl. Mech. (ASME) 47, 266-272.

Hossain, M. R. (2005). "FE Modeling of The Stress-Strain Behavior of Sand in Cyclic Plane Strain Loading", B. Sc. Engg. Thesis, Bangladesh University Of Engineering and Technology.

Hossain, M.R., Siddiquee, M.S.A, Tatsuoka, F, (2005), "Development Of A Cyclic Model For Pressure Insensitive Soil", Proceedings of the Japan Bangladesh Joint Seminar on Advances in Bridge Engineering, August, 2005, Dhaka

Khoei, A.R. and Jamali, N. (2004), "On The Implementation of A Multi-Surface Kinematic Hardening Plasticity and its Applications", International Journal of Plasticity Volume 21, Issue 9, September 2005, 1741-1770

Konder, R.L. (1963), "Hyperbolic stress-strain response: cohesive soils", Journal of Soil Mechanics and Foundation Division, ASCE, 89(SM1), 115-143, 1963.

Krieg., R.D., Kreig., D.B., 1977. Accuracies of numerical solution methods for the elastic and perfectly plastic model. J. Pr. Vess. Tech., Transactions of the ASME, 510-515.

Lemaitre, J., Chaboche, J.(1990), "Mechanics of solid materials", Cambridge University Press

Masuda, T., Tatsuoka, F., Yamada, S. and Sato, T. (1999), "Stress strain behavior of sand in plane strain compression, extension and cyclic loading tests", Soils Found., 39(5), 31-45.

Montáns, F. J. (2000). "Bounding surface plasticy model with extended Masing's behavior", Comput. Methods Appl. Mech. Engrg., 182, 135-162

Mróz, Z., "On the Description of Anisotropic Workhardening," J. Mech. Phys. Solids, 15, 163.

Nayak, G.C. and O.C. Zienkiewicz. (1972), Elastic-Plastic Stress Analysis: A Generalization for Various Consitutive Relations Including Strain Softening. Int. J. Num. Meth. Engrg., Vol. 5, No. 1, pp. 113-125.

Ohno, N. and Wang, J.D., (1993), "Kinematic Hardening Rules With Critical State Of Dynamic Recovery, Part I: Formulation And Basic Features For Ratchetting Behavior", International Journal of Plasticity, Vol. 9, pp. 375-390

Ohno, N., Abdel Karim, M., 2000, Uniaxial ratcheting of 316FR steel at room temperature part II: Constitutive modeling and simulation, ASME J. Appl. Mech. 122, 35-41.

Ohno, N., and Wang, J.D. (1991), "Transformation of a Nonlinear Kinematic Hardening Rule to a Multisurface Form Under Isothermal and Nonisothermal Conditions," Int. J. Plasticity, 7, 879.

Ortiz, M. and Simo, J. C. (1986)."An analysis of a new class of integration algorithms for elasto plastic constitutive relation", Int. J. Numer. Meth. Engeg., Vol 23, 353-366.

Ortiz, M., Popov, E.P., 1985. Accuracy and stability of integration algorithms for elasto-plastic constitutive relations. Int. J. Numer. Meth. Engg. 21, 1561-1576.

Otter, J. R. H. (1965), "Computation of Prestressed Concrete Reactor Pressure Vessels Using Dynamic Relaxation", Nuclear Structural Engineering, 1, 61-75

Papadrakakis, M (1981), "A Method for the Automatic Evaluation of the Dynamic Relaxation parameters", Computer Methods in Applied Mechanics and Engineering, 25, 35-48.

Prager, W. (1956), " A New Method of Analyzing Stresses and Strains in Work Hardening Plastic Solids", J. Appl. Mech., 23, 795-810.

Ramm. E. et al. (1981), "Strategies for Tracing the Nonlinear Response Near Limit Points", Nonlinear Finite Element Analysis in Structural Mechanics, 63-83.

Riks, E. (1979), "An Incremental Approach to the solution of Snapping and Buckling Problems", International Journal of Solids and Structures, 15, 529-551.

Rushton K. R. (1968), "Dynamic Relaxation Solutions of Elastic Plate Problems", Journal of Strain Analysis, 3, 23-32.

Saenz, L. P. (1964), "Discussion of Equation for the Stress-Strain Curve of Concrete by Desayi and Krishman." J. Am. Concr. Inst., Vol. 61, September, pp. 1229-1235.

Schofield, A. N., and P. Wroth (1968), "Critical State Soil Mechanics", McGraw-Hill, New York.

Siddiquee, M. S. A. (1994). "FEM simulations of deformation and failure of stiff geomaterials based on element test results", D. Eng. dissertation, The University of Tokyo.

Simo, J.C. and R.L. Taylor. (1986), A Consistent Return Mapping Algorithm for Plane Strain Elastoplasticity. Int. J. Num. Meth. Engrg., Vol. 22, pp. 649-670.

Tanak, T., "Elasto-plastic strain hardening-softening soil model with shear banding".

Tatsuoka, F., Masuda, T., Siddiquee, M. S. A. and Koseki, J. (2003), "Modeling the stress strain relations of sand in cyclic plane strain loading", Journal of Geotechnical and Geoenvironmental Engineering, ASCE, May, 2003

Tatsuoka, F., Siddiquee, M. S. A., Park, C. S., Sakamoto, M. and Abe, F. (1993), "Modeling stress-strain relations of sand", Soils and Foundations, Vol. 33, No. 2, 60-81, June 1993.

Turner, M. J., Clough, R. W., Martin, H. C. and Topp, L. J. (1956), "Stiffness and Deslection Analysis of Comples Structures", Journal of Aero. Sci., 23, 805-823.

Underwood, P. (1983). "Dynamic Relaxation", Computational methods for transient analysis, Belytschko, T. and Hughes, T. J. R., eds., 245-265.

Valanis, K. C. (1971), "A Theory of Viscoplasticity without a Yield Surface, I: General Theory; II: Application to Mechanical Behavior of Metals", Arch. Mech., Vol. 23, No. 4, pp. 517-551.

Vremeer, P. A. (1978). "A double hardening model for sand", Geotechnique, 28, No. 4, 413-433.

Welsh, A. K. (1967), "Discoussion on Dynamic Relaxation" Proceedings of Institute of Civil Engineers, 37, 723-750.

Wempner, G. A. (1971), "Discrete Approximations Related to Nonlinear Theories of Solids", International Journal of Solids and Structures, 7, 1581-1599.

Wilkins, M.L., 1964. Calculation of elastic-plastic flow. In methods of Computational Physics (Edited by Alder et.al.). Academia Press, New York.

APPENDIX-A: DEFINATIONS

ε_{ij}	Total strain
ε_{ij}^{e}	Elastic strain
ε_{ij}^{p}	Plastic strain
e_{ij}	Deviatoric total strain
ε_{v}	Volumetric total strain, $\varepsilon_v = \varepsilon_1 + \varepsilon_2 + \varepsilon_3$
α_{ij}	Kinematic hardening variable
η	A model variable
C	Instantaneous slope of the $\alpha_{ij} \sim \varepsilon_{ij}^{p}$ relationship
$\sin\varphi_{mob}$	Mobilized angle of friction, $\sin\varphi_{mob} = (\sigma_1 - \sigma_3)/(\sigma_1 + \sigma_3)$
γ	Shear strain, $\gamma = \varepsilon_1 - \varepsilon_3$
R	Stress ratio, $R = \sigma_1/\sigma_3$
κ	Internal plastic variable
D	Drag parameter
A	Material parameter
D	Stress-dilatancy relationship
σ_{ij}	Total stress
S_{ij}	Deviatoric stress
P	Hydrostatic pressure, $p = (\sigma_1 + \sigma_2 + \sigma_3)/3$
D_{ijkl}^{e}	Elastic matrix
f	Yield function
λ	Magnitude of incremental plastic strain
K^{e}	Bulk modulus of elasticity
G	Shear modulus of elasticity
P	Vector of internal forces
P^{init}	Vector of nodal forces due to initial stresses
F	vector of external forces
B	displacement-strain transformation matrix

N	number of elements in the FEM discretization
ve	Volume of the each element
m	mass matrix
c	damping matrix
$\ddot{u}$	acceleration vector
$\dot{u}$	velocity vector

APPENDIX-B

B1. Derivatives of the Yield Functions

B1.1 Pressure Independent Model

$$\frac{\partial f}{\partial \sigma_{kl}} = \frac{S_{ij} - \alpha_{ij}}{\sqrt{(S_{ij} - \alpha_{ij}):(S_{ij} - \alpha_{ij})}}$$

$$\frac{\partial f}{\partial \kappa} = C.\frac{\partial f}{\partial \sigma_{kl}}.\frac{\partial f}{\partial \sigma_{kl}}$$

B1.1 Pressure Dependent Model

$$\frac{\partial f}{\partial S_{ij}} = \frac{S_{ij} - p\alpha_{ij}}{\sqrt{(S_{ij} - p\alpha_{ij}):(S_{ij} - p\alpha_{ij})}}$$

$$\frac{\partial f}{\partial \kappa} = -p\frac{S_{ij} - p\alpha_{ij}}{\sqrt{(S_{ij} - p\alpha_{ij}):(S_{ij} - p\alpha_{ij})}}.C.\frac{\partial f}{\partial S_{ij}}$$

$$\frac{\partial f}{\partial p} = -\frac{\alpha_{ij}.(S_{ij} - p\alpha_{ij})}{\sqrt{(S_{ij} - p\alpha_{ij}):(S_{ij} - p\alpha_{ij})}}$$

B.2 Linear quadrilateral element

Displacements (u,v) in a plane element are interpolated from nodal displacements (u_i,v_i) using shape function N_i as follows:

$$\begin{Bmatrix} u \\ v \end{Bmatrix} = \begin{bmatrix} \mathrm{N}_1 & 0 & \mathrm{N}_2 & 0 & \ldots \\ 0 & \mathrm{N}_1 & 0 & \mathrm{N}_2 & \ldots \end{bmatrix} \begin{Bmatrix} u_1 \\ v_1 \\ u_2 \\ v_2 \\ . \\ . \\ . \end{Bmatrix}$$

$$\Rightarrow \underline{\underline{u}} = \underline{\underline{\mathrm{N}d}}$$

Where, $\underline{\underline{N}}$ is the shape function matrix, $\underline{\underline{u}}$ the displacement vector and $\underline{\underline{d}}$ the nodal displacement vector.

From strain-displacement relation, the strain vector is:

$$\underline{\underline{\varepsilon}} = \underline{\underline{Du}}$$

$$\Rightarrow \quad \underline{\underline{\varepsilon}} = \underline{\underline{DNd}}$$

$$\Rightarrow \quad \underline{\underline{\varepsilon}} = \begin{bmatrix} \frac{\partial}{\partial x} & 0 \\ 0 & \frac{\partial}{\partial y} \\ \frac{\partial}{\partial y} & \frac{\partial}{\partial x} \end{bmatrix} \begin{bmatrix} N_1 & 0 & N_2 & 0 & N_3 & 0 & N_4 & 0 \\ 0 & N_1 & 0 & N_2 & 0 & N_3 & 0 & N_4 \end{bmatrix} \begin{bmatrix} u_1 \\ v_1 \\ u_2 \\ v_2 \\ u_3 \\ v_3 \\ u_4 \\ v_4 \end{bmatrix}$$

$$\Rightarrow \quad \underline{\underline{\varepsilon}} = \underline{\underline{Bd}}$$

Where, $\underline{\underline{B}}$ is the strain-displacement matrix.

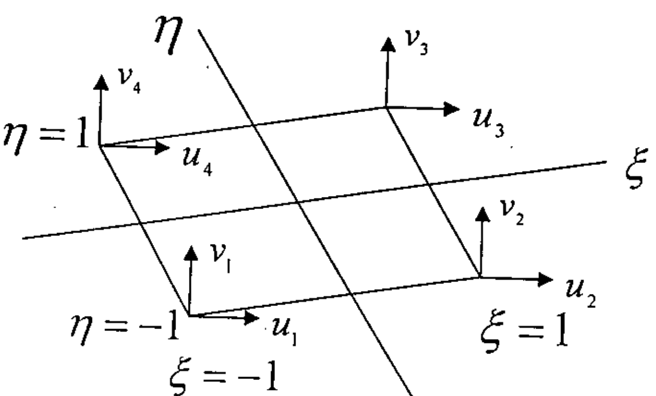

Figure B.1: Linear quadrilateral element

In the natural coordinate system (ξ, η), the four shape functions are,

$$N_1 = \frac{1}{4}(1-\xi)(1-\eta)$$

$$N_2 = \frac{1}{4}(1+\xi)(1-\eta)$$

$$N_3 = \frac{1}{4}(1+\xi)(1+\eta)$$

$$N_4 = \frac{1}{4}(1-\xi)(1+\eta)$$

For one point integration, at $(0,0)$ coordinate, $N_1 = N_2 = N_3 = N_4 = 1/4$.

So, the $\underline{\underline{B}}$ matrix becomes,

$$\underline{\underline{B}} = \frac{1}{2}\begin{bmatrix} -1/B & 0 & 1/B & 0 & 1/B & 0 & -1/B & 0 \\ 0 & -1/L & 0 & -1/L & 0 & 1/L & 0 & 1/L \\ 0 & 0 & 0 & 0 & 0 & 0 & 0 & 0 \\ -1/L & -1/B & -1/L & 1/B & 1/L & 1/B & 1/L & -1/B \\ 0 & 0 & 0 & 0 & 0 & 0 & 0 & 0 \\ 0 & 0 & 0 & 0 & 0 & 0 & 0 & 0 \end{bmatrix}$$

Where B and L are dimensions of the quadrilateral element.

B.3 Numerical integration – Gauss quadrature

The most obvious way of obtaining the integral,

$$I = \int_{-1}^{1}\int_{-1}^{1} f(\xi,\eta)\,d\xi\,d\eta$$

or, $$I = \sum_{i=1}^{n}\sum_{j=1}^{n} H_i H_j f(\xi_j,\eta_i)$$

For one point integration $\xi_j = 0, \eta_i = 0$, $n = 1$ and $H_i = H_j = 2$.

So, $$w_i = H_i H_j = 4$$

Thus, we can calculate the nodal force vector,

$$P = \sum_{N} \int_{ve} B^T \sigma dv$$

or, $$P = 4B^T\sigma$$